Abnormal spindle-like microcephaly-associated (ASPM) mutations strongly disrupt neocortical structure but spare the hippocampus and long-term memory

Sandrine Passemard, Alain Verloes, Thierry Billette de Villemeur, Odile Boespflug-Tanguy, Karen Hernandez, Marion Laurent, Bertrand Isidor, Corinne Alberti, Nathalie Pouvreau, Séverine Drunat, et al.

Abnormal spindle-like microcephaly-associated (*ASPM*) mutations strongly disrupt neocortical structure but spare the hippocampus and long-term memory

Sandrine Passemard (1-4), Alain Verloes (1-3), Thierry Billette de Villemeur (1,5-6), Odile Boespflug (1,2,4), Karen Hernandez (3), Marion Laurent (7), Bertrand Isidor (8), Corinne Alberti (2,9), Nathalie Pouvreau (3), Séverine Drunat (1, 3), Bénédicte Gérard (3), Vincent El Ghouzzi (1,2), Jorge Gallego (1,2), Monique Elmaleh-Bergès (1,2,10), Wieland B. Huttner (11), Stephan Eliez (12), Pierre Gressens* (1,2,4,13), Marie Schaer* (12,14).

* These authors contributed equally to this work

(1) Inserm, U1141, Hôpital Robert Debré, Paris, France

(2) Université Paris Diderot – Sorbonne Paris Cité, Paris, France

(3) Département de Génétique, Hôpital Robert Debré, AP-HP, Paris, France

(4) Service de Neuropédiatrie, Hôpital Robert Debré, AP-HP, Paris, France

(5) Sorbonne Universités, UPMC Université Paris 06, Paris, France

(6) Service de Neuropédiatrie, Hôpital Trousseau, AP-HP, Paris, France

(7) Service de Psychopathologie, Hôpital Robert Debré, AP-HP, Paris, France

(8) Service de Génétique, Hôpital Mère-Enfant, Nantes, France

(9) Inserm CIC-EC1426, Hôpital Robert Debré, AP-HP, Paris, France

(10) Service de Radiopédiatrie, Hôpital Robert Debré, AP-HP, Paris, France

(11) Max Planck Institute of Molecular Cell Biology and Genetics, Dresden, Germany

(12) Office Médico-Pédagogique, Département de psychiatrie, Université de Genève, Suisse

(13) Center for Developing Brain, King's College, St. Thomas' Campus, London, United Kingdom

(14) Stanford Cognitive & Systems Laboratory, Stanford University School of Medicine,

Palo Alto, California, USA

Corresponding author:

Sandrine Passemard

Address: Inserm U1141, Hôpital Robert Debré, 48 boulevard Sérurier, 75019 Paris, France

sandrine.passemard@inserm.fr

Phone: +33 (0)1 40 03 36 91, Fax: +33 (0)1 40 03 22 77

Running title: Brain structure and memory in ASPM microcephaly

ABSTRACT

Autosomal recessive primary microcephaly results from abnormal brain development linked to proliferation defects in neural progenitors. The most frequent form, caused by *ASPM* mutations, is usually defined by a reduced brain volume and is associated with intellectual disability. Although many *ASPM* cases have now been reported, structural brain abnormalities and their link with cognitive disabilities have been rarely investigated. In this study, we used high resolution T1-weighted magnetic resonance imaging in seven patients with *ASPM* mutations and 39 healthy age-matched controls to quantify regional volumes, thickness, surface area, gyrification index and white matter volumes of 30 cortical regions. We observed a consistent reduction of 50% or more in the volume and surface area of all cortical regions except for the hippocampus and surrounding medial temporal structures, which were significantly less reduced. Neuropsychologic assessment indicated significant impairments of cognitive abilities. However, these impairments were associated with normal mnesic abilities, in keeping with the relative preservation of the hippocampus and medial temporal structures. These results show that, contrary to current opinion, the cortical volume and surface area of patients with *ASPM* mutations is reduced depending on a regionally specific fashion and their cognitive profile reflects this heterogeneity. The precise characterization of the cortical map and cognitive abilities of patients with *ASPM* mutations should allow developing more focused reeducative interventions well-suited to their real abilities.

Keywords:

Brain development, human cerebral cortex, hippocampus, MCPH, memory

Abbreviations:

ANOVA: Analysis Of Variance

aRGcs: apical Radial Glial cells

APs: apical progenitors

ASPM: Abnormal Spindle Microcephaly associated

bRGcs: basal Radial Glial cells

BPs: basal progenitors

CMS: Children's Memory Scale

CTRL: Control group

CSF: Cerebrospinal Fluid

FSIQ: Full scale IQ

IQ: Intelligence Quotient

lGI: local Gyrification Index

MCPH: Autosomal recessive primary microcephaly

MEM: Wechsler Memory Scale-III

NECs: Neurepithelial cells

OFC: Occipitofrontal circumference

ROIs: Regions-Of-Interest

SD: Standard Deviation

SEM: Standard Error of the Mean

SVZ: SubVentricular Zone

VZ: Ventricular Zone

WAIS-III: Wechsler Adult Intelligence Scale-III

WISC IV: Wechsler Intelligence Scale for Children-IV

1. Introduction

Microcephaly represents the most common clinical sign of various developmental disorders of the brain (Barkovich, Kuzniecky et al., 2005), with a prevalence of about 2% worldwide (Van Den Bosch, 1959). Microcephaly is characterized by a decrease in brain size that is indirectly reflected by a decrease of occipitofrontal circumference (OFC) that is more than two standard deviations (SD) below normal values for age and sex, and is closely associated with intellectual disability (Passemard, Kaindl et al. 2013). Genetic forms of primary microcephaly (collectively known as MicroCephaly Primary Hereditary or MCPH), are very rare, genetically heterogeneous disorders with a recessive inheritance, and considered model diseases for impaired brain growth. The incidence of MCPH is estimated at 1-3/100 000 births in Western countries, and is probably ten times higher in the Indian subcontinent (Szabo, Pap et al., 2010; Woods, Bond et al., 2005). MCPH patients usually display normal or slightly delayed motor development, mild-to-moderate intellectual disability, and in a minority of cases, mild pyramidal signs and late onset epilepsy (Kaindl, Passemard et al., 2009). Microcephaly, always present at birth, may already be detectable by the second trimester of gestation.

MCPH is caused by a reduction in the number of neural progenitors undergoing proliferation possibly associated with increased apoptosis among these progenitors (Gilmore and Walsh, 2013; Kaindl, Passemard et al., 2009; Thornton and Woods, 2009; Verloes, Drunat et al., 2013). In mouse models of MCPH, this decrease results in a variable reduction in the volume, surface area and/or thickness of the cerebral cortex, depending on the MCPH gene involved (Gruber, Zhou et al., 2011; Lizarraga, Margossian et al., 2010; Passemard, El Ghouzzi et al., 2011; Pulvers, Bryk et al., 2010).

In humans, MCPH can result from mutations in at least thirty genes that nevertheless explain less than half the cases in Western countries (for review, see (Verloes, Drunat et al., 2013). Of

these, mutations in the *ASPM* (Abnormal spindle-like, microcephaly associated) gene cause MCPH5, the most frequent genetic form of MCPH, especially in Pakistan (Bond, Roberts et al., 2002). *ASPM* is known to contribute to the genetic basis of brain evolution in humans and other primates (Evans, Anderson et al., 2004; Kouprina, Pavlicek et al., 2004; Mekel-Bobrov, Gilbert et al., 2005; Montgomery and Mundy, 2013). Mouse *Aspm* is expressed in the ventricular zone (VZ) of the neocortex during neurogenesis (Bond, Roberts et al., 2002; Fish, Kosodo et al., 2006). It encodes a protein associated with the centrosome (Bond et al., 2002) and the midbody (Paramasivam, Chang et al., 2007) that, by participating in spindle pole positioning in apical progenitor cells, allows them to maintain symmetric divisions (Fish, Kosodo et al., 2006).

ASPM mutations cause a global reduction in brain volume in humans that is usually not associated with major cerebral malformations. So far, MRI data have been published for only 12 among the 200 reported families with *ASPM* mutations (Bond, Roberts et al., 2002; Desir, Cassart et al., 2008; Passemard, Titomanlio et al., 2009). Hypoplastic frontal lobes have been described in a single patient with an *ASPM* mutation (Desir, Cassart et al., 2008), suggesting that the reduction in brain volume may be non-homogeneous, with some regions being more affected than others. But no quantitative description, according to region of the cortical reduction in volume/thickness and surface area has been reported in these microcephalic patients. It is thus still unclear whether the cortical map is maintained in patients with *ASPM* mutations, or if some cortical regions are less preserved than others.

In addition to the scarcity of information on cerebral and cortical structures in MCPH patients, the impact of MCPH mutations on cognitive development remains obscure. Mild to severe cognitive or behavioral deficits have been identified in patients with *ASPM* mutations in previous studies (Bond, Roberts et al., 2002; Bond, Scott et al., 2003; Desir, Cassart et al., 2008; Hu, Suckow et al., 2014; Kumar, Blanton et al., 2004; Muhammad, Mahmood Baig et

al., 2009; Nicholas, Swanson et al., 2009; Sajid Hussain, Marriam Bakhtiar et al., 2013; Shen, Eyaid et al., 2005; Tan, del Gaudio et al., 2013). However, the systematic cognitive evaluation of these patients has not been reported so far. The magnitude of their cognitive impairments is thus still undetermined and the possibility that MCPH patients with *ASPM* mutations may have conserved cognitive abilities in some domains despite the overall reduction in brain volume should be considered.

Here, we aimed to determine how these small brains are organized structurally and to what extent they are functionally impaired in a genetically homogeneous cohort of patients with mutations in the *ASPM* gene. To this end, we combined quantitative neuroimaging using T1-weighted anatomical imaging with neuropsychological assessment. We used a region-based approach to measure changes in cortical volume, surface area and thickness, white matter volume, as well as gyrification index in seven patients ranging in age from 7 to 24 years, to test the hypothesis that patients with *ASPM* mutations would display regional differences in brain volume reduction and in cortical area patterning. In addition, we asked whether any structural differences revealed by neuroimaging would differentially impact cognitive outcome.

2. MATERIALS and METHODS

2.1 Participants

Patients:

Seven microcephalic male patients with *ASPM* mutations, ranging in age from 7 to 24 years, were recruited in this study. All patients were right-handed. Clinical and mutational data are summarized in Table 1. OFCs of the patients are given in the Supplementary Figure 1A.

Patients, and their parents if they were younger than 18 years old, provided informed consent to participate. The protocol was favorably reviewed by the ethical committee of Paris.

Healthy controls:

Age-matched controls (CTRL) included 39 healthy right-handed male subjects, aged from 6 to 25 years and paired by age with patients. The distribution of the subjects according to age is shown in Supplementary Figure 1B. Control participants had no past or present history of neurological or psychiatric diseases. The control group had an average full scale IQ of 109.8 ±12.34 SD. Written informed consent was obtained from all subjects, as well as the parents of subjects younger than 18 years of age, in accordance with protocols approved by the Institutional Review Board of the Geneva University School of Medicine.

2.2 Imaging

Cerebral magnetic resonance images were acquired with a T1-weighted 3D volumetric pulse sequence on a 1.5 Tesla Philips scanner (Gyroscan Intera 1.5 T, Philips Medical Systems, Best, The Netherlands) at the time of cognitive evaluation (or within a few weeks). The MRI dataset consisted of a series of 124 coronal slices with a voxel size of 0.94 x 0.94 x 1.5 mm (TR = 35ms, TE = 6ms, flip angle = 45°). Image processing was carried out using published algorithms included in the FreeSurfer software (http://surfer.nmr.mgh.harvard.edu). Briefly, the processing consisted of the exclusion of non-brain tissue, the automatic segmentation of subcortical grey matter structures, and the extraction of cortical surfaces (Fischl, Liu et al., 2001). Both intensity and continuity information from the entire 3D MR volume were used in segmentation and deformation procedures, thus generating an accurate representation of cortical thickness and volumes. These procedures have been validated with histological studies (Rosas, Liu et al., 2002) and shown to be reliable across scanner manufacturers and field strengths (Han, Jovicich et al., 2006). At the end of the reconstruction process, the

following volumes were available: estimated intracranial [cerebral and cerebellar tissue and ventricles], supratentorial [total intracranial volume except the cerebellum and brain stem] and infratentorial [cerebellum (grey matter and white matter) and brain stem], total cerebral grey [including cortical, subcortical and cerebellar grey matter] and white matter [cerebral and cerebellar white matter], brain stem, cerebellum [grey and white matter], and the volumes of subcortical structures including the thalamus, putamen, pallidum and caudate nucleus, as well as the amygdala, nucleus accumbens, ventral diencephalon, substantia nigra and hippocampus.

2.3 Regional cortical volumes

After cortical reconstruction, the cortex was also subdivided into cortical gyral regions as described by Desikan et al. (Desikan, Segonne et al., 2006). This parcellation method, based on major sulci, has been shown to be both valid and reliable, with high intra-class correlation coefficients between the manual and automated procedures for both cortical volume estimates and regional boundaries. Parcellation produces 34 regions subdivided into 11 frontal regions, 9 temporal regions, 5 parietal regions, 4 occipital regions, 4 regions of the cingulate cortex, and the insula. The frontal pole and the banks of the superior temporal sulcus were excluded from statistical analyses, as both are small regions with relatively poor reliability. Cortical volume was therefore estimated for 31 regions-of-interest (ROIs) in each hemisphere and for each subject (10 frontal regions, 8 temporal regions, 5 parietal regions, 4 occipital regions, 4 regions of the cingulate cortex) and the insula. We carefully checked the cortical reconstructions for each participant. Even for the smallest patients' brain, a voxel size of 0.94 x 0.94 x 1.5 mm allowed an adequate delineation of the anatomic curvature of the cortex. The inter-subject registration and parcellation into gyral regions was also checked for each participant. The pattern of cerebral sulci in patients with *ASPM* mutations being mostly simplified but with the preservation of the primary sulci, the delineation of the 32 cortical

regions was not particularly affected by the absence of some secondary or tertiary sulci (see some examples of cortical parcellation in Supplementary Figure 2).

Lobar volumes were computed by summing the volumes of the cortical regions corresponding to each of the four main lobes (frontal, parietal, temporal, occipital) and to the regions corresponding to the cingulate cortex.

2.4 Cortical thickness, surface area and cortical gyrification

Cortical thickness was measured in the native space of the images, as the shortest distance between the white (grey-white boundary) and the pial (grey-CSF interface) surfaces. As a result, cortical thickness values with submillimeter accuracy were available for more than 150 000 points in each hemisphere. Finally, based on the outer cortical surface reconstruction (pial surface), local Gyrification Index (lGI) was measured at thousands of points across each hemisphere using previously validated algorithms (Schaer, Cuadra et al., 2008). lGI is a surface-based measurement of the degree of cortical folding that iteratively quantifies the amount of cortex buried within the sulcal folds in the surrounding circular region.

2.5 Regional white matter volumes

The parcellation of the cortex was subsequently used to subdivide the underlying white matter volume as described in (Salat, Greve et al., 2009). Briefly, a Voronoi diagram was created in the white matter voxels based on the distance to the nearest parcellation label, using a distance constraint of 5 mm. At the end of this process, regional white matter volumes were available for the 30 regions corresponding to the aforementioned cortical labels.

2.6 Cognitive assessment

Intellectual abilities of patients and healthy controls were assessed using the recommended Wechsler scale at the time of assessment.

Patients

The Intelligence Quotient (IQ) was assessed between 2009 and 2013 using the Wechsler Adult Intelligence Scale-III (Wechsler, 1997) or the Wechsler Intelligence Scale for Children-IV (Wechsler, 2003) according to age (WISC IV: 6 to 16 years, n=2; WAIS-III after the age of 16 years, n=3). Two patients (Patients 6 and 7) could not participate in the neuropsychological assessment. The pregnant mother of patient 7 had learned of the recurrence of microcephaly in her fetus and did not wish her son to contribute to the evaluation at that time. Patient 6 was too hyperkinetic and restless to be assessed with the Wechsler scales.

Full Scale IQ (FSIQ) was calculated from four scores: a verbal score (Verbal Comprehension Index, VCI), a visual or visuospatial scale with the use of materials (Perceptual Organisation Index, POI), a score of mental manipulation of data (Working Memory Index, WMI) and a score of graphic processing speed (Processing Speed Index, PSI). The 4 scores are independent and involve specific cognitive abilities such as lexical stock, general knowledge, verbal comprehension and verbal reasoning (VCI); visuomotor and visuospatial skills to examine a problem, organize thoughts and find solutions using cubes or pictures (POI); short-term memory, concentration abilities, mental manipulation, planning abilities, cognitive flexibility, arithmetic reasoning (WMI) and finally performance speed in graphic realization and visual discrimination (PSI).

Memory was assessed by the Wechsler Memory Scale-III (Wechsler, 1998) and the Children's Memory Scale (Cohen, 1997) depending on age (CMS: 5 to 16 years, n=2; MEM after the age of 16 years, n=3). These scales consist of different memory mechanisms: immediate memory and delayed memory with respect to both verbal and visual modalities, and the process of learning and delayed recognition.

Healthy controls

The Intelligence Quotient (IQ) was assessed between 2002 and 2009 using the Wechsler Adult Intelligence Scale-III (Wechsler, 1997) or the Wechsler Intelligence Scale for Children-III (Wechsler, 1991) according to age (WISC III: 6 to 16 years, n=29; WAIS-III after the age of 16 years, n=10). Full scale IQ (FSIQ), Verbal Comprehension Index and Perceptual Organisation Index were calculated from the subtests as recommended for all subjects. Working memory IQ and processing speed IQ were available for subjects who were evaluated using the WAIS-III scale. Memory was assessed as for patients.

2.7 Statistical analysis:

Imaging analysis:

Based on histological and structural-MRI studies that provided information on dynamic regional and age-related changes in the volume and thickness of grey matter and in the volume of white matter in developing children and adolescents (Chouinard-Decorte, McKay et al., 2014; Franke, Ziegler et al., 2010; Giedd, Blumenthal et al., 1999; Giedd, Stockman et al., 2010; Gogtay, Giedd et al., 2004; Lenroot and Giedd, 2006; Raznahan, Lerch et al., 2011; Sowell, Thompson et al., 2001), we divided our participant samples into 3 age groups (6-11.9, 12-17.9 and 18-25 years). The raw data for intracranial and cerebral cortex volumes are indicated in Supplementary Figure1 C-D. To take into account age-related differences in cortical volumes as detailed below, all volumes in both groups were expressed as a percentage of the average of the controls of the corresponding age group ± SEM.

We compared the differences in the volume data between microcephalic patients with *ASPM* mutations and controls. To investigate whether the decrease in cortical volume was similar in the different lobes, we analyzed the volume of the frontal, parietal, occipital and temporal lobes and cingulate cortex. Within each hemisphere, we measured the volumes of 31 specific

cortical and underlying white matter regions and, finally, the thickness and surface area of 30 cortical regions as previously defined (Desikan, Segonne et al., 2006).

All variables were analyzed by a repeated-measures two-way ANOVA (GraphPad Prism 5.0), with genotype (controls versus patients) as a between-subject factor, and lobes or regions as within-subject factors (since volume, thickness and area are measured in the same subjects (Lew, 2007)). Topographical differences in the effects of the *ASPM* mutations were investigated through genotype-by-lobe or genotype-by-region interaction analyses. A significant genotype-by-region interaction indicates/means that differences between patients and controls depend on the region. Whenever ANOVA revealed statistically significant interactions for lobes or specific regions, partial pairwise comparisons were conducted with a post hoc test (using the Bonferroni correction for multiple comparisons) in order to identify regional differences in patients as compared to controls. In all analyses, a statistical threshold of $p<0.05$ indicated significance (uncorrected for multiple comparisons).

Cognitive analysis:

Within the group of patients, general intellectual abilities (Full Scale IQ, Verbal IQ, Performance IQ, Processing Speed IQ and Working Memory IQ) and mnesic abilities (Immediate or Delayed Auditory/Verbal Memory and Immediate or Delayed Visual Memory) were compared to search for specific learning disorders using a one-way ANOVA followed by a Bonferroni post hoc test if specific differences were observed among scores. In all analyses, a statistical threshold of $p<0.05$ indicated significance.

The results of the Wechsler tests in controls were used merely to establish the validity of this group for structural analyses (i.e. to ensure that they were normal) and were not compared to those of patients.

3. Results

3.1 Brain volume is reduced by half in patients with *ASPM* mutations and this reduction differentially affects brain regions

Mean values ± SEM of global brain volumes are presented in Supplementary Table 1. The intracranial volume was strongly reduced in patients as compared to controls (~45% of that in controls, Figure 1A, i.e. a 55% volume reduction). This effect was supported by a significant reduction of supratentorial and infratentorial volumes ($p<0.0001$ for both comparisons, Figure 1A). However, the volume reduction was stronger in the supratentorial compartment than in the infratentorial compartment in patients as compared to controls (~45% vs 67 % of that in controls, respectively, i.e. a 55% vs 33% volume reduction) as supported by the significant genotype-by-region interaction (F 75.45, dF 2;88, $p<0.0001$) and the partial pairwise comparisons shown in Figure 1A. Within the infratentorial compartment, the reduction in volume was not uniform in patients as compared to controls (Figure 1B), with the cerebellar volume significantly better preserved than that of the brainstem (~ 70% vs 58% of that in controls respectively, i.e. a 30% vs 42% volume reduction), as supported by the significant genotype-by-region interaction (F 21.96, dF 1;44, $p<0.0001$) and the partial pairwise comparisons (Figure 1B). Similarly, the reduction in volume in patients was higher in the total white matter of the brain than in the total grey matter, as shown by the significant genotype-by-region interaction (F 9.74, dF 1;44, $p=0.0032$) and the partial pairwise comparisons (Figure 1C). Finally, the cortical grey matter was more affected than the subcortical or cerebellar grey matter in patients as compared to controls (~ 45%, 64% and 70% of that in controls respectively, i.e. a 55%, 36% and 30% volume reduction) as supported by the significant genotype-by-region interaction (F 57.2, dF 2;88, $p<0.0001$) and the partial pairwise comparisons (Figure 1E). In contrast, *ASPM* mutations caused a similar volume

reduction on the cortex and on the underlying white matter (genotype-by-region interaction: ns, Figure 1E).

Taken together, these data indicate that, in our series, *ASPM* deficiency strongly reduces the cerebral cortical grey and underlying white matter volumes by over 50% and has a lesser impact on the subcortical grey matter and cerebellum.

3.2 Neocortical areas - but not the hippocampus - are strongly reduced in patients with *ASPM* mutations

Within each lobe, the cortical volume was strongly reduced in patients as compared to controls (Figure 2A-B). However, this reduction was not similar across lobes in the right hemisphere, as supported by the significant genotype-by-region interaction (Supplementary Table 2A) and the pairwise comparisons (Figure 2B). The reduction in volume was significantly higher in the right cingulate cortex than in the right frontal, parietal and temporal cortices in patients as compared to controls. To determine whether this reduction in the cortical volume was similar in all cortical regions in patients as compared to controls, we carried out a more detailed analysis within each lobe. Mean values ± SEM of the 31 regional cortical volumes are presented in Supplementary Table 2B.

Parietal, occipital and cingulate regions

In both hemispheres, *ASPM* mutations caused a similar volume reduction in regions of parietal, occipital lobes and cingulate cortex (genotype-by-region interaction: ns, Supplementary Table 2B).

Frontal regions

We observed a significant regional effect of the *ASPM* mutations on frontal cortical volumes as supported by the significant genotype-by-region interaction (Supplementary Tables 2A) and the partial pairwise comparisons (Supplementary Figure 3). In the left hemisphere, the

volume of the paracentral cortex (premotor cortex and supplementary motor cortex, in orange in Figure 2C) or pars opercularis (Broca's area, in yellow in Figure 2C) was better preserved than that of the caudal middle frontal (posterior part of the dorsolateral prefrontal cortex) or of the rostral middle frontal cortices (anterior part of the dorsolateral prefrontal cortex, in red in Figure 2C). Within the right hemisphere, pars opercularis was significantly higher in volume than the prefrontal regions (caudal/rostral middle frontal, lateral or medial orbitofrontal cortices (Figure 2C, Supplementary Figure 3C-D).

Temporal regions

We observed a regional effect of *ASPM* mutations on temporal cortical volumes, as supported by the significant genotype-by-region interaction (Supplementary Tables 2A) and the partial pairwise comparisons (Figure 3). The cortical volume of the medial temporal structures including the entorhinal and parahippocampal cortices and the hippocampus was significantly better preserved than that of the five other temporal regions (Figure 2C and Figure 3A-B). This difference was highly significant in the bilateral parahippocampal cortex and hippocampus and in the right entorhinal cortex when compared to other regions of the temporal lobes (Figure 3C-F).

Together, these data indicate that, in our series, the hippocampus and surrounding medial temporal structures display a relatively preserved volume when compared to the extreme decrease in the volume of all neocortical areas in both hemispheres in patients with *ASPM* mutations.

3.3 The decrease in cortical volume is associated with regional increases in cortical thickness

Since the cortical volume is the product of thickness x surface area (Im, Lee et al., 2008), we sought to determine whether or not the reduction in cortical volume in the absence of *ASPM*

was due to decreased cortical thickness in the regions analyzed above. We observed a regional effect of *ASPM* mutations on cortical thickness within each lobe, as supported by the significant genotype-by-region interaction (Supplementary Table 2A) and the pairwise comparisons (Supplementary Figures 4 and 5), except for the right temporal lobe and the left cingulum. Mean values ± SEM of the 30 regional cortical thickness are presented in Supplementary Table 2B.

Occipital, temporal and cingulate regions

Only two regions of significant decreased cortical thickness were observed in these lobes in patients as compared to controls. These regions (highlighted in green in Figure 4) were located in the cuneus within the left occipital lobe and in the rostral anterior cingulate cortex within the right cingulate region (see also Supplementary Figure 4A, F). No difference in cortical thickness was observed between patients and controls in the temporal lobes (Figure 4 and Supplementary Figure 4 C-D). A few clusters of increased cortical thickness, shown in dark blue in Figure 4, were observed within the right occipital lobe (pericalcarine cortex and lingual gyrus) and cingulate regions (left caudal anterior cingulate cortex, isthmus regions bilaterally, Supplementary Figure 4 B, E-F) in patients as compared to controls.

Frontal and parietal regions

Surprisingly, several frontal and parietal cortical regions were significantly thicker in patients than in controls in both hemispheres, as supported by the significant genotype-by-region interaction (Supplementary Table 2A) and the pairwise comparisons shown in Supplementary Figures 5. Indeed, significant increased cortical thickness was observed in the pars opercularis bilaterally, in the rostral middle frontal, lateral orbitofrontal, pars orbitalis of the left frontal lobe, as well as in the right caudal middle frontal region (in dark blue in Figure 4, see also Supplementary Figure 5A-D).

The cortex was also significantly thicker bilaterally in all parietal regions in patients as compared to controls, except for the left precuneus and the right supramarginal gyrus (in blue green or light blue in Figure 4, see also Supplementary Figure 5 E-H).

Together, these data indicate that the observed decrease in cortical volume in patients with *ASPM* mutations, in our series, is not due to a decrease in cortical thickness. On the contrary, the cerebral cortex is thicker in the prefrontal cortex, inferior frontal gyrus and parietal regions lining the Sylvian fissure and the postcentral sulcus, especially in the left hemisphere.

3.4 The reduction in cortical volume in patients with *ASPM* mutations is accounted for by a decrease in surface area

As the reduction in cortical volume was not related to a decrease in cortical thickness in most regions examined, we investigated whether this reduction in volume could be due to decreased surface area. We measured the surface area of the same regions as above. We observed an extreme and homogeneous reduction of the surface area of all lobes in patients as compared to controls in both hemispheres. In the right hemisphere, this reduction was not similar across lobes as supported by the genotype-by-region interaction (Supplementary Table 2A) and the pairwise comparisons shown in Figure 5B. The reduction in cortical surface area was significantly higher in the cingulate cortex than in the frontal, parietal and temporal lobes in patients as compared to controls (Figure 5B). Mean values ± SEM of the 30 regional cortical surface area are presented in Supplementary Table 2B.

Frontal, parietal, occipital and cingulate regions

The cortical surface area of most regions of the frontal, parietal, occipital and cingulate lobes in both hemispheres depicted in Figure 5 as was strongly reduced in patients as compared to controls. We did not find any genotype-by-region interaction for the parietal, occipital and cingulate lobes and the right frontal lobe (Supplementary Table 2A). *ASPM* mutations had a

very mild regional effect on surface area of the left frontal lobe as supported by the genotype-by-region interaction (Supplementary Tables 2A) and the partial pairwise comparisons shown in Supplementary Figure 6 C-D. The precentral and pars opercularis regions (depicted in orange in Figure 5) were lightly higher in terms of surface area than the caudal and rostral middle frontal regions (depicted in dark red in Figure 5) in patients as compared to controls (see also Supplementary Figure 6A-B).

Temporal regions

We observed a significant regional effect of *ASPM* mutations on temporal cortical surface area as supported by the significant genotype-by-region interaction (Supplementary Table 2A) and the partial pairwise comparisons (Supplementary Figures 6 E-H). As for volume measurements, the surface area of the parahippocampal cortices and of the left entorhinal cortex, depicted in green or yellow in Figure 5, was significantly higher than that of the five other temporal regions (middle, transverse, inferior temporal cortex or fusiform region, depicted in red or dark red in Figure 5) in both hemispheres in patients as compared to controls (see also Supplementary Figure 6 E-H).

Taken together, these data suggest that the surface area of various cortical regions is reduced to the same extent as their volume in patients with *ASPM* mutations as compared to controls, except for the parahippocampal and entorhinal cortices, which are significantly more preserved.

3.5 The volumes of the cerebral cortex and the underlying cortical white matter are reduced in similar proportions

To assess the impact of the loss of cortical volume on the underlying white matter, we measured white matter volume in all regions.

A strong reduction in the subcortical white matter volume was observed in patients as compared to controls throughout the frontal, parietal, occipital and temporal lobes and cingulate regions (Figure 6 A-B), without genotype-by-lobe interaction (Supplementary Table 3A). However, upon further examination of the regions within each lobe, we detected a significant regional effect of the *ASPM* mutations on the temporal lobes, as demonstrated by the significant genotype-by-region interaction (Supplementary Tables 3B) and the pairwise comparisons (Figure 6 C-D). Mean values ± SEM of the 30 regional white matter volumes are presented in Supplementary Table 3B. Within the temporal lobes, significantly more preserved white matter regions were located exclusively in the medial temporal lobes in patients as compared to controls. As in the cerebral cortex, the regions with the least reduction in the volume of the white matter in patients were in the parahippocampal cortici and in the right entorhinal cortex (Figure 6C-D).

These data indicate that regions that are more preserved in volume at cortical levels are also preserved at the white matter level.

3.6 The Gyrification Index is reduced in patients with *ASPM* mutations and this reduction differentially affects cortical regions

Mean values ± SEM of the lGI of the 30 cortical regions are presented in Supplementary Table 4A. The local Gyrification Index (lGI) was significantly reduced in patients as compared to controls in all part of the cortex as shown in Figure 7. However, this reduction was not similar across regions, as supported by the significant genotype-by-region interaction (Supplementary Table 4A), and the pairwise comparisons (Supplementary Tables 4C) except for the left parietal lobe. Regions with the higher lGI (Figure 7) were located within the frontal lobes (paracentral, superior frontal, medial orbitofrontal regions), the temporal lobes (inferior temporal region, entorhinal and parahippocampal cortices) and cingulate regions

(rostral and caudal anterior cingulate and posterior cingulate regions). At the opposite, pars opercularis and superior temporal bilaterally were regions with the lower lGI (Figure 7).

These data suggest that *ASPM* deficiency disrupts the gyrification with regional variations. Exploratory correlation analysis between lGI and surface area, thickness or volume did not reveal significant relationship.

3.7 Patients with *ASPM* mutations display preserved mnesic capacities but mildly reduced or borderline intellectual abilities

Neuropsychological tests could be performed in five patients. All patients had mild to moderate intellectual deficiency (mean FSIQ 51.2 ± 6.5), with an impairment of their language skills (Verbal Comprehension Index = 60.6 ± 11.4, limited lexical stock, but most importantly, difficulties with verbal or conceptual reasoning), and of their visuomotor or visuospatial analysis (Perceptual Organisation Index = 57.2 ± 9.1). They also displayed deficits in the memorization of new information, had significant difficulties with arithmetic and problem solving (Working Memory Index = 54.2 ± 4), and were very slow at performing graphical tasks (Processing Speed Index = 59.4 ± 13.2) (Figure 8 and Supplementary Table 5).

In contrast, and despite this global cognitive disability, in the domain of memory function, all patients had a mean score in the normal range or at the limits of normality for verbal tasks (immediate verbal memory = 82.80 ± 11.86), and more particularly for visual tasks (immediate visual memory = 90.2 ± 12.03). Their abilities in encoding/learning can be mobilized with a low rate of forgetting in delayed memory at recall tasks (delayed verbal memory= 75.6 ± 16.26 and especially delayed visual memory = 85.8 ± 6.4); these differences were very significant ($p<0.001$ for each of the four comparisons for FSIQ versus immediate (or delayed) verbal (or visual) memory)). No difference was observed between mnesic

processes (immediate and delayed memory) regardless of the type of memory tested (auditory-verbal or visual memory).

These data reveal that patients with *ASPM* mutations in our series have mild intellectual disability, but all of them have preserved memory functions and learning abilities.

4. DISCUSSION

Our study demonstrates that *ASPM* loss-of-function mutations in microcephalic patients disrupt cortical and white matter development in a region-specific fashion. The 50% reduction in cortical volume is the result of a decrease in cortical expansion mainly in terms of surface area, although this is partially counterbalanced by a regional increase in cortical thickness. The volume of the cerebellum and subcortical grey matter was relatively spared when compared to the cerebral cortex and underlying white matter. Within the cortex, the volume of the hippocampus, surrounding medial temporal structures and the underlying white matter was preserved compared to other regions of the neocortex. In keeping with the relative integrity of the hippocampus, the mnesic abilities of patients with *ASPM* mutations were preserved despite their intellectual disabilities. These results provide strong evidence for a regional variation in the reduction of brain volume and significant differences in cortical arealization in these patients that could influence their cognitive functions.

Global reduction in brain volume

The brain volume of MCPH patients is reduced by definition, but to our knowledge, no study has quantified this reduction region-wise. Here, we show that the reduction in the brain volume of patients with *ASPM* mutations affects the cortex and the underlying white matter to a greater extent than the subcortical grey matter and cerebellum. Murine *Aspm* gene is expressed in the ventricular zone of the pallium (Bond, Roberts et al., 2002; Fish, Kosodo et

al., 2006). In humans, recent data have shown that *ASPM* is expressed in the VZ, inner and outer subventricular zone (i and oSVZ) (Fietz, Lachmann et al., 2012), and in apical and basal radial glial cells (Florio, Albert et al., 2012) of the pallium. In line with this pattern of expression, our data show that *ASPM* mutations affect structures derived from the pallium to a greater extent than those derived from the subpallium, the diencephalon, the mesencephalon or the rhombencephalon.

Cortical regionalization

Our study highlights a differential reduction in several cortical regions in patients as compared to controls, rather than a homogeneous cortical reduction, suggesting that *ASPM* mutations disrupt cortical and white matter development in a regionally specific fashion. Regional differences in cortical patterning, in particular the regulation of the expression gradients of specific morphogens and their influence on brain size and cortical arealization, have been previously described in both animals and humans (Arai and Pierani, 2014; Bartley, Jones et al., 1997; Bishop, Goudreau et al., 2000; Chen, Fiecas et al., 2013; Chen, Gutierrez et al., 2012; Lohmann, von Cramon et al., 1999; Mallamaci, Muzio et al., 2000; O'Leary, Chou et al., 2007). However, there is increasing evidence that the genetic contribution to cortical regionalization or gyrification is linked to a differential rather than a uniform process of cortical expansion (Chen, Panizzon et al., 2011; Fei, Haffner et al., 2014; Florio, Albert et al., 2015; Lukaszewicz, Cortay et al., 2006; Ronan, Voets et al., 2013; Stahl, Walcher et al., 2013). One could thus envisage that the differential expression of *ASPM* at either the cellular or the regional level or differences in the region-specific rate of proliferation of progenitors expressing *ASPM* could result in locoregional variations in cortical expansion. Whereas genetic factors have been demonstrated to influence the establishment of regionalization, extrinsic factors such as thalamocortical axons are known to impose functional arealization (Miyashita-Lin, Hevner et al., 1999; Rakic, 1988). Since white matter volumes also differ

according to region in patients with *ASPM* mutations, it is conceivable that in the absence of ASPM, changes in peripheral sensory inputs also regulate the dimensions of cortical areas.

Volume/surface/thickness/gyrification relationship

The present study provides evidence that cortical volume, surface area and the gyrification index are significantly decreased in patients with *ASPM* mutations while cortical thickness is maintained or locally increased in some regions. This indicates that in the absence of ASPM, there is not enough lateral/tangential cortical expansion and folding, but intact or locally increased radial expansion. The 3D growth in volume of the cerebral cortex is closely related to its surface and thickness components as well as to its folding. The radial expansion (i.e. increase in thickness) and tangential expansion (i.e. increase in surface area) of the future cortex occur concomitantly and depend on the balance between the proliferation and differentiation of the progenitor pool within a limited window of time i.e. neurogenesis (Rakic, 2009). The tangential expansion of the cerebral cortex is the result first of the amplification of neurepithelial cells (NECs) and apical Radial Glial cells (aRGcs), which undergo symmetric proliferative divisions within the VZ (Florio and Huttner, 2014; Gotz and Huttner, 2005; Stancik, Navarro-Quiroga et al., 2010; Taverna, Gotz et al., 2014), and later during neurogenesis, of the amplification of basal Radial Glial cells (bRGcs). *Aspm* is expressed in apical progenitors (AP; which include the aRGcs) of the VZ and is necessary to maintain their symmetric divisions in mice (Fish, Dehay et al., 2008; Fish, Kosodo et al., 2006). The differential regional amplification of basal progenitors (BPs; including bRGc and basal Intermediate Progenitors or bIPs), which form a large population in the outer SVZ of gyral species such as ferrets, primates and humans (Betizeau, Cortay et al., 2013; Fietz, Kelava et al., 2010; Garcia-Moreno, Vasistha et al., 2012; Hansen, Lui et al., 2010; LaMonica, Lui et al., 2013; Lui, Hansen et al., 2011), is sufficient to drive cortical surface area expansion and gyrification even in lissencephalic species such as mice (Florio, Albert et

al., 2015; Nonaka-Kinoshita, Reillo et al., 2013; Rash, Tomasi et al., 2013; Stahl, Walcher et al., 2013). The hypothesis put forward by Sun and Hevner in a recent review is that bRGcs may expand the cortical plate tangentially whereas bIPs primarily amplify neuron number to "fill in" the cortical layers that have been thinned out by tangential expansion (Sun and Hevner, 2014). In keeping with this hypothesis, our findings suggest that *ASPM* loss-of-function mutations may lead to a reduction in the amplification not only of the pool of APs but also of BPs (bRGcs rather than bIPs). However, this remains a hypothesis and needs to be verified by studying the pattern of expression of *ASPM* in humans during neurogenesis and analyzing fetuses carrying *ASPM* mutations.

Cognition

Five of the seven patients were assessed using Wechsler neuropsychological tests. Our results show that despite their mild-to-moderate intellectual disabilities, patients with *ASPM* mutations have preserved mnesic abilities. These findings are consistent with the protection of the volume of their hippocampus and medial temporal structures (entorhinal and parahippocampal cortices). Both the grey and white matter of medial temporal regions are significantly protected compared to other neocortical regions in patients with *ASPM* mutations, suggesting possible interconnections between these structures and other cortical regions required for memory retrieval. Our data demonstrate objectively and quantifiably what other studies have previously suggested based on either partial, or non homogeneous neuropsychological evaluations (Desir, Cassart et al., 2008; Kumar, Blanton et al., 2004; Passemard, Titomanlio et al., 2009) the absence of formal assessments (Bond, Roberts et al., 2002; Bond, Scott et al., 2003; Desir, Cassart et al., 2008; Hu, Suckow et al., 2014; Kumar, Blanton et al., 2004; Muhammad, Mahmood Baig et al., 2009; Nicholas, Swanson et al., 2009; Sajid Hussain, Marriam Bakhtiar et al., 2013; Shen, Eyaid et al., 2005; Tan, del Gaudio et al., 2013). As a rule, higher IQ is associated with higher grey and white matter volumes in

all lobes (Haier, Jung et al., 2004; Posthuma, De Geus et al., 2002). Typically, the strongest correlations with IQ involve frontal grey matter volumes (Haier, Jung et al., 2004; Sowell, Thompson et al., 2001), which are strongly reduced in our patients. Intelligence is linked to dynamic changes in the thickness and surface area of the human cortex during childhood and adolescence: children and adolescents with higher IQ show cortical thinning and surface expansion (Karama, Colom et al., 2011; Schnack, van Haren et al., 2014). This is concordant with the reverse observation in our patients. A large number of studies support the role of medial temporal structures, most notably the hippocampus, in episodic memory, in concert with the parahippocampal, perirhinal and entorhinal cortices (Eichenbaum, 2004; Quiroga; Squire, Stark et al., 2004; Squire, Wixted et al., 2007). Because long-term memory is still functional in patients with *ASPM* mutations, promoting, maintaining and improving their ability to learn would be of great interest.

Our study aimed to provide new data concerning brain structure in ASPM microcephaly that could help extend our understanding of the role of ASPM in human brain development. To our knowledge, regional changes in cortical volume, surface, thickness and gyrification have never been analyzed so far in MCPH patients. Our analysis of variance shows that each *ASPM* mutation significantly reduces brain size, supporting the assumption that ASPM plays a role in brain development, and that this effect depends significantly on the region under study, as shown by the genotype-by-region interactions. A limitation of the present study is the small cohort size, although the reported data are all statistically significant. Considering that OFC (ranging from -3.5 to -7.5 SD) appear to be reduced to a lower extent than in other studies (Bond, Scott et al., 2003), one could reasonably ask whether this cohort is representative of patients with *ASPM* mutations. However, it should be remembered that our patients are on

average younger than in other cohorts and we expect their OFC to worsen with age (Supplementary Figure 1A and (Passemard, Titomanlio et al., 2009).

5. CONCLUSION

Our findings show that despite the mild intellectual disability caused by the reduction of the volume and surface area of their neocortex, patients with *ASPM* mutations exhibit a relative sparing of the volume/surface area of the hippocampus and surrounding medial temporal structures as well as preserved mnesic abilities. These results highlight how *ASPM* loss-of-function mutations could affect neocortical and hippocampal development and reveal a link between genetics and cognitive behavior in microcephaly.

6. FUNDING

This work was supported by grants from the « Fondation pour la Recherche Médicale (FRC) », the « Programme Hospitalier de Recherche Clinique (PHRC), grant agreement n° P100128 / IDRCB : 2010-A01481-38" and ERA-NET E-Rare-2 2013, grant agreement n° ANR-13-RARE-0007-01 2013. MS was supported by a grant from the National Center of Competence in Research (NCCR) "SYNAPSY—The Synaptic Bases of Mental Diseases" financed by the Swiss National Science Foundation, and by a fellowship from the Swiss National Foundation of Science (#145760).

7. ACKNOWLEDGEMENTS

The authors would like to thank Dr Catherine Verney for discussions and critical reading of the manuscript, Jeannette Nardelli for discussions and S. Rasika for reading and carefully correcting this manuscript.

REFERENCES

ARAI Y and PIERANI A. Development and evolution of cortical fields. *Neurosci Res, 2014*.

BARKOVICH AJ, KUZNIECKY RI, JACKSON GD, GUERRINI R, and DOBYNS WB. A developmental and genetic classification for malformations of cortical development. *Neurology,* 65: 1873-87, 2005.

BARTLEY AJ, JONES DW, and WEINBERGER DR. Genetic variability of human brain size and cortical gyral patterns. *Brain,* 120 (Pt 2): 257-69, 1997.

BETIZEAU M, CORTAY V, PATTI D, PFISTER S, GAUTIER E, BELLEMIN-MENARD A, AFANASSIEFF M, HUISSOUD C, DOUGLAS RJ, KENNEDY H, and DEHAY C. Precursor diversity and complexity of lineage relationships in the outer subventricular zone of the primate. *Neuron,* 80: 442-57, 2013.

BISHOP KM, GOUDREAU G, and O'LEARY DD. Regulation of area identity in the mammalian neocortex by emx2 and pax6. *Science,* 288: 344-9, 2000.

BOND J, ROBERTS E, MOCHIDA GH, HAMPSHIRE DJ, SCOTT S, ASKHAM JM, SPRINGELL K, MAHADEVAN M, CROW YJ, MARKHAM AF, WALSH CA, and WOODS CG. Aspm is a major determinant of cerebral cortical size. *Nat Genet,* 32: 316-20, 2002.

BOND J, SCOTT S, HAMPSHIRE DJ, SPRINGELL K, CORRY P, ABRAMOWICZ MJ, MOCHIDA GH, HENNEKAM RC, MAHER ER, FRYNS JP, ALSWAID A, JAFRI H, RASHID Y, MUBAIDIN A, WALSH CA, ROBERTS E, and WOODS CG. Protein-truncating mutations in aspm cause variable reduction in brain size. *Am J Hum Genet,* 73: 1170-7, 2003.

CHEN CH, FIECAS M, GUTIERREZ ED, PANIZZON MS, EYLER LT, VUOKSIMAA E, THOMPSON WK, FENNEMA-NOTESTINE C, HAGLER DJ, JR., JERNIGAN TL, NEALE MC, FRANZ CE, LYONS MJ, FISCHL B, TSUANG MT, DALE AM, and KREMEN WS. Genetic topography of brain morphology. *Proc Natl Acad Sci U S A,* 110: 17089-94, 2013.

CHEN CH, GUTIERREZ ED, THOMPSON W, PANIZZON MS, JERNIGAN TL, EYLER LT, FENNEMA-NOTESTINE C, JAK AJ, NEALE MC, FRANZ CE, LYONS MJ, GRANT MD, FISCHL B, SEIDMAN LJ, TSUANG MT, KREMEN WS, and DALE AM. Hierarchical genetic organization of human cortical surface area. *Science,* 335: 1634-6, 2013.

CHEN CH, PANIZZON MS, EYLER LT, JERNIGAN TL, THOMPSON W, FENNEMA-NOTESTINE C, JAK AJ, NEALE MC, FRANZ CE, HAMZA S, LYONS MJ, GRANT MD, FISCHL B, SEIDMAN LJ, TSUANG MT, KREMEN WS, and DALE AM. Genetic influences on cortical regionalization in the human brain. *Neuron,* 72: 537-44, 2011.

CHO ZH, HAN JY, HWANG SI, KIM DS, KIM KN, KIM NB, KIM SJ, CHI JG, PARK CW, and KIM YB. Quantitative analysis of the hippocampus using images obtained from 7.0 t mri. *Neuroimage,* 49: 2134-40, 2010.

CHOUINARD-DECORTE F, MCKAY DR, REID A, KHUNDRAKPAM B, ZHAO L, KARAMA S, RIOUX P, SPROOTEN E, KNOWLES E, KENT JW, JR., CURRAN JE, GORING HH, DYER TD, OLVERA RL, KOCHUNOV P, DUGGIRALA R, FOX PT, ALMASY L, BLANGERO J, BELLEC P, EVANS AC, and GLAHN DC. Heritable changes in regional cortical thickness with age. *Brain Imaging Behav,* 8: 208-16, 2014.

COHEN. Children's memory scale. . *San Antonio, TX: The Psychological Corporation*, 1997.

DAGER SR, WANG L, FRIEDMAN SD, SHAW DW, CONSTANTINO JN, ARTRU AA, DAWSON G, and CSERNANSKY JG. Shape mapping of the hippocampus in young children with autism spectrum disorder. *AJNR Am J Neuroradiol,* 28: 672-7, 2007.

DESIKAN RS, SEGONNE F, FISCHL B, QUINN BT, DICKERSON BC, BLACKER D, BUCKNER RL, DALE AM, MAGUIRE RP, HYMAN BT, ALBERT MS, and KILLIANY RJ. An automated labeling system for subdividing the human cerebral cortex on mri scans into gyral based regions of interest. *Neuroimage,* 31: 968-80, 2006.

DESIR J, CASSART M, DAVID P, VAN BOGAERT P, and ABRAMOWICZ M. Primary microcephaly with aspm mutation shows simplified cortical gyration with antero-posterior gradient pre- and post-natally. *Am J Med Genet A,* 146A: 1439-43, 2008.

EICHENBAUM H. Hippocampus: Cognitive processes and neural representations that underlie declarative memory. *Neuron,* 44: 109-20, 2004.

EVANS PD, ANDERSON JR, VALLENDER EJ, GILBERT SL, MALCOM CM, DORUS S, and LAHN BT. Adaptive evolution of aspm, a major determinant of cerebral cortical size in humans. *Hum Mol Genet,* 13: 489-94, 2004.

FEI JF, HAFFNER C, and HUTTNER WB. 3' utr-dependent, mir-92-mediated restriction of tis21 expression maintains asymmetric neural stem cell division to ensure proper neocortex size. *Cell Rep,* 7: 398-411, 2014.

FIETZ SA, KELAVA I, VOGT J, WILSCH-BRAUNINGER M, STENZEL D, FISH JL, CORBEIL D, RIEHN A, DISTLER W, NITSCH R, and HUTTNER WB. Osvz progenitors of human and ferret neocortex are epithelial-like and expand by integrin signaling. *Nat Neurosci,* 13: 690-9, 2010.

FIETZ SA, LACHMANN R, BRANDL H, KIRCHER M, SAMUSIK N, SCHRODER R, LAKSHMANAPERUMAL N, HENRY I, VOGT J, RIEHN A, DISTLER W, NITSCH R, ENARD W, PAABO S, and HUTTNER WB. Transcriptomes of germinal zones of human and mouse fetal neocortex suggest a role of extracellular matrix in progenitor self-renewal. *Proc Natl Acad Sci U S A,* 109: 11836-41, 2012.

FISCHL B, LIU A, and DALE AM. Automated manifold surgery: Constructing geometrically accurate and topologically correct models of the human cerebral cortex. *IEEE Trans Med Imaging,* 20: 70-80, 2001.

FISH JL, DEHAY C, KENNEDY H, and HUTTNER WB. Making bigger brains-the evolution of neural-progenitor-cell division. *J Cell Sci,* 121: 2783-93, 2008.

FISH JL, KOSODO Y, ENARD W, PAABO S, and HUTTNER WB. Aspm specifically maintains symmetric proliferative divisions of neuroepithelial cells. *Proc Natl Acad Sci U S A,* 103: 10438-43, 2006.

FLORIO M, ALBERT M, TAVERNA E, NAMBA T, BRANDL H, LEWITUS E, HAFFNER C, SYKES A, WONG FK, PETERS J, GUHR E, KLEMROTH S, PRUFER K, KELSO J, NAUMANN R, NUSSLEIN I, DAHL A, LACHMANN R, PAABO S, and HUTTNER WB. Human-specific gene arhgap11b promotes basal progenitor amplification and neocortex expansion. *Science,* 347: 1465-70, 2015.

FLORIO M and HUTTNER WB. Neural progenitors, neurogenesis and the evolution of the neocortex. *Development,* 141: 2182-94, 2014.

FRANKE K, ZIEGLER G, KLOPPEL S, and GASER C. Estimating the age of healthy subjects from t1-weighted mri scans using kernel methods: Exploring the influence of various parameters. *Neuroimage,* 50: 883-92, 2010.

GARCIA-MORENO F, VASISTHA NA, TREVIA N, BOURNE JA, and MOLNAR Z. Compartmentalization of cerebral cortical germinal zones in a lissencephalic primate and gyrencephalic rodent. *Cereb Cortex,* 22: 482-92, 2012.

GIEDD JN, BLUMENTHAL J, JEFFRIES NO, CASTELLANOS FX, LIU H, ZIJDENBOS A, PAUS T, EVANS AC, and RAPOPORT JL. Brain development during childhood and adolescence: A longitudinal mri study. *Nat Neurosci,* 2: 861-3, 1999.

GIEDD JN, STOCKMAN M, WEDDLE C, LIVERPOOL M, ALEXANDER-BLOCH A, WALLACE GL, LEE NR, LALONDE F, and LENROOT RK. Anatomic magnetic resonance imaging of the developing child and adolescent brain and effects of genetic variation. *Neuropsychol Rev,* 20: 349-61, 2010.

GILMORE EC and WALSH CA. Genetic causes of microcephaly and lessons for neuronal development. *Wiley Interdiscip Rev Dev Biol,* 2: 461-78, 2013.

GOGTAY N, GIEDD JN, LUSK L, HAYASHI KM, GREENSTEIN D, VAITUZIS AC, NUGENT TF, 3RD, HERMAN DH, CLASEN LS, TOGA AW, RAPOPORT JL, and THOMPSON PM. Dynamic mapping of human cortical development during childhood through early adulthood. *Proc Natl Acad Sci U S A,* 101: 8174-9, 2004.

GOTZ M and HUTTNER WB. The cell biology of neurogenesis. *Nat Rev Mol Cell Biol,* 6: 777-88, 2005.

GRUBER R, ZHOU Z, SUKCHEV M, JOERSS T, FRAPPART PO, and WANG ZQ. Mcph1 regulates the neuroprogenitor division mode by coupling the centrosomal cycle with mitotic entry through the chk1-cdc25 pathway. *Nat Cell Biol,* 13: 1325-34, 2011.

HAIER RJ, JUNG RE, YEO RA, HEAD K, and ALKIRE MT. Structural brain variation and general intelligence. *Neuroimage,* 23: 425-33, 2004.

HAN X, JOVICICH J, SALAT D, VAN DER KOUWE A, QUINN B, CZANNER S, BUSA E, PACHECO J, ALBERT M, KILLIANY R, MAGUIRE P, ROSAS D, MAKRIS N, DALE A, DICKERSON B, and FISCHL B. Reliability of mri-derived measurements of human cerebral cortical thickness: The effects of field strength, scanner upgrade and manufacturer. *Neuroimage,* 32: 180-94, 2006.

HANSEN DV, LUI JH, PARKER PR, and KRIEGSTEIN AR. Neurogenic radial glia in the outer subventricular zone of human neocortex. *Nature,* 464: 554-561, 2010.

HOPKINS RO, ABILDSKOV TJ, BIGLER ED, and WEAVER LK. Three dimensional image reconstruction of neuroanatomical structures: Methods for isolation of the cortex, ventricular system, hippocampus, and fornix. *Neuropsychol Rev,* 7: 87-104, 1997.

HU H, SUCKOW V, MUSANTE L, ROGGENKAMP V, KRAEMER N, ROPERS HH, HUBNER C, WIENKER TF, and KAINDL AM. Previously reported new type of autosomal recessive primary microcephaly is caused by compound heterozygous aspm gene mutations. *Cell Cycle,* 13: 1650-1, 2014.

IM K, LEE JM, LYTTELTON O, KIM SH, EVANS AC, and KIM SI. Brain size and cortical structure in the adult human brain. *Cereb Cortex,* 18: 2181-91, 2008.

KAINDL AM, PASSEMARD S, KUMAR P, KRAEMER N, ISSA L, ZWIRNER A, GERARD B, VERLOES A, MANI S, and GRESSENS P. Many roads lead to primary autosomal recessive microcephaly. *Prog Neurobiol*, 2009.

KARAMA S, COLOM R, JOHNSON W, DEARY IJ, HAIER R, WABER DP, LEPAGE C, GANJAVI H, JUNG R, and EVANS AC. Cortical thickness correlates of specific cognitive performance accounted for by the general factor of intelligence in healthy children aged 6 to 18. *Neuroimage,* 55: 1443-53, 2011.

KOUPRINA N, PAVLICEK A, MOCHIDA GH, SOLOMON G, GERSCH W, YOON YH, COLLURA R, RUVOLO M, BARRETT JC, WOODS CG, WALSH CA, JURKA J, and LARIONOV V. Accelerated evolution of the aspm gene controlling brain size begins prior to human brain expansion. *PLoS Biol,* 2: E126, 2004.

KUMAR A, BLANTON SH, BABU M, MARKANDAYA M, and GIRIMAJI SC. Genetic analysis of primary microcephaly in indian families: Novel aspm mutations. *Clin Genet,* 66: 341-8, 2004.

LAMONICA BE, LUI JH, HANSEN DV, and KRIEGSTEIN AR. Mitotic spindle orientation predicts outer radial glial cell generation in human neocortex. *Nat Commun,* 4: 1665, 2013.

LENROOT RK and GIEDD JN. Brain development in children and adolescents: Insights from anatomical magnetic resonance imaging. *Neurosci Biobehav Rev,* 30: 718-29, 2006.

LEW M. Good statistical practice in pharmacology. Problem 2. *Br J Pharmacol,* 152: 299-303, 2007.

LIZARRAGA SB, MARGOSSIAN SP, HARRIS MH, CAMPAGNA DR, HAN AP, BLEVINS S, MUDBHARY R, BARKER JE, WALSH CA, and FLEMING MD. Cdk5rap2 regulates

centrosome function and chromosome segregation in neuronal progenitors. *Development,* 137: 1907-17, 2010.

LOHMANN G, VON CRAMON DY, and STEINMETZ H. Sulcal variability of twins. *Cereb Cortex,* 9: 754-63, 1999.

LUI JH, HANSEN DV, and KRIEGSTEIN AR. Development and evolution of the human neocortex. *Cell,* 146: 18-36, 2011.

LUKASZEWICZ A, CORTAY V, GIROUD P, BERLAND M, SMART I, KENNEDY H, and DEHAY C. The concerted modulation of proliferation and migration contributes to the specification of the cytoarchitecture and dimensions of cortical areas. *Cereb Cortex,* 16 Suppl 1: i26-34, 2006.

MALLAMACI A, MUZIO L, CHAN CH, PARNAVELAS J, and BONCINELLI E. Area identity shifts in the early cerebral cortex of emx2-/- mutant mice. *Nat Neurosci,* 3: 679-86, 2000.

MEKEL-BOBROV N, GILBERT SL, EVANS PD, VALLENDER EJ, ANDERSON JR, HUDSON RR, TISHKOFF SA, and LAHN BT. Ongoing adaptive evolution of aspm, a brain size determinant in homo sapiens. *Science,* 309: 1720-2, 2005.

MIYASHITA-LIN EM, HEVNER R, WASSARMAN KM, MARTINEZ S, and RUBENSTEIN JL. Early neocortical regionalization in the absence of thalamic innervation. *Science,* 285: 906-9, 1999.

MONTGOMERY SH and MUNDY NI. Evolution of aspm is associated with both increases and decreases in brain size in primates. *Evolution,* 66: 927-32, 2012.

MUHAMMAD F, MAHMOOD BAIG S, HANSEN L, SAJID HUSSAIN M, ANJUM INAYAT I, ASLAM M, ANVER QURESHI J, TOILAT M, KIRST E, WAJID M, NURNBERG P, EIBERG H, TOMMERUP N, and KJAER KW. Compound heterozygous aspm mutations in pakistani mcph families. *Am J Med Genet A,* 149A: 926-930, 2009.

NICHOLAS AK, SWANSON EA, COX JJ, KARBANI G, MALIK S, SPRINGELL K, HAMPSHIRE D, AHMED M, BOND J, DI BENEDETTO D, FICHERA M, ROMANO C, DOBYNS WB, and WOODS CG. The molecular landscape of aspm mutations in primary microcephaly. *J Med Genet,* 46: 249-53, 2009.

NONAKA-KINOSHITA M, REILLO I, ARTEGIANI B, MARTINEZ-MARTINEZ MA, NELSON M, BORRELL V, and CALEGARI F. Regulation of cerebral cortex size and folding by expansion of basal progenitors. *EMBO J,* 32: 1817-28, 2013.

O'LEARY DD, CHOU SJ, and SAHARA S. Area patterning of the mammalian cortex. *Neuron,* 56: 252-69, 2007.

PARAMASIVAM M, CHANG YJ, and LOTURCO JJ. Aspm and citron kinase co-localize to the midbody ring during cytokinesis. *Cell Cycle,* 6: 1605-12, 2007.

PASSEMARD S, EL GHOUZZI V, NASSER H, VERNEY C, VODJDANI G, LACAUD A, LEBON S, LABURTHE M, ROBBERECHT P, NARDELLI J, MANI S, VERLOES A, GRESSENS P, and LELIEVRE V. Vip blockade leads to microcephaly in mice via disruption of mcph1-chk1 signaling. *J Clin Invest,* 12:3071-3087, 2011.

PASSEMARD S, KAINDL AM, and VERLOES A. Microcephaly. *Handb Clin Neurol,* 111: 129-41, 2013.

PASSEMARD S, TITOMANLIO L, ELMALEH M, AFENJAR A, ALESSANDRI JL, ANDRIA G, DE VILLEMEUR TB, BOESPFLUG-TANGUY O, BURGLEN L, DEL GIUDICE E, GUIMIOT F, HYON C, ISIDOR B, MEGARBANE A, MOOG U, ODENT S, HERNANDEZ K, POUVREAU N, SCALA I, SCHAER M, GRESSENS P, GERARD B, and VERLOES A. Expanding the clinical and neuroradiologic phenotype of primary microcephaly due to aspm mutations. *Neurology,* 73: 962-9, 2009.

POSTHUMA D, DE GEUS EJ, BAARE WF, HULSHOFF POL HE, KAHN RS, and BOOMSMA DI. The association between brain volume and intelligence is of genetic origin. *Nat Neurosci,* 5: 83-4, 2002.

PULVERS JN, BRYK J, FISH JL, WILSCH-BRAUNINGER M, ARAI Y, SCHREIER D, NAUMANN R, HELPPI J, HABERMANN B, VOGT J, NITSCH R, TOTH A, ENARD W, PAABO S, and HUTTNER WB. Mutations in mouse aspm (abnormal spindle-like microcephaly associated) cause not only microcephaly but also major defects in the germline. *Proc Natl Acad Sci U S A,* 107: 16595-600, 2010.

QUIROGA RQ. Concept cells: The building blocks of declarative memory functions. *Nat Rev Neurosci,* 13: 587-97, 2012.

RAKIC P. Specification of cerebral cortical areas. *Science,* 241: 170-6, 1988.

RAKIC P. Evolution of the neocortex: A perspective from developmental biology. *Nat Rev Neurosci,* 10: 724-35, 2009.

RASH BG, TOMASI S, LIM HD, SUH CY, and VACCARINO FM. Cortical gyrification induced by fibroblast growth factor 2 in the mouse brain. *J Neurosci,* 33: 10802-14, 2013.

RAZNAHAN A, LERCH JP, LEE N, GREENSTEIN D, WALLACE GL, STOCKMAN M, CLASEN L, SHAW PW, and GIEDD JN. Patterns of coordinated anatomical change in human cortical development: A longitudinal neuroimaging study of maturational coupling. *Neuron,* 72: 873-84, 2011.

RONAN L, VOETS N, RUA C, ALEXANDER-BLOCH A, HOUGH M, MACKAY C, CROW TJ, JAMES A, GIEDD JN, and FLETCHER PC. Differential tangential expansion as a mechanism for cortical gyrification. *Cereb Cortex,* 24: 2219-28, 2013.

ROSAS HD, LIU AK, HERSCH S, GLESSNER M, FERRANTE RJ, SALAT DH, VAN DER KOUWE A, JENKINS BG, DALE AM, and FISCHL B. Regional and progressive thinning of the cortical ribbon in huntington's disease. *Neurology,* 58: 695-701, 2002.

SAJID HUSSAIN M, MARRIAM BAKHTIAR S, FAROOQ M, ANJUM I, JANZEN E, REZA TOLIAT M, EIBERG H, KJAER KW, TOMMERUP N, NOEGEL AA, NURNBERG P, BAIG SM, and HANSEN L. Genetic heterogeneity in pakistani microcephaly families. *Clin Genet,* 83: 446-51, 2013.

SALAT DH, GREVE DN, PACHECO JL, QUINN BT, HELMER KG, BUCKNER RL, and FISCHL B. Regional white matter volume differences in nondemented aging and alzheimer's disease. *Neuroimage,* 44: 1247-58, 2009.

SCHAER M, CUADRA MB, TAMARIT L, LAZEYRAS F, ELIEZ S, and THIRAN JP. A surface-based approach to quantify local cortical gyrification. *IEEE Trans Med Imaging,* 27: 161-70, 2008.

SCHNACK HG, VAN HAREN NE, BROUWER RM, EVANS A, DURSTON S, BOOMSMA DI, KAHN RS, and HULSHOFF POL HE. Changes in thickness and surface area of the human cortex and their relationship with intelligence. *Cereb Cortex,* 2014.

SHEN J, EYAID W, MOCHIDA GH, AL-MOAYYAD F, BODELL A, WOODS CG, and WALSH CA. Aspm mutations identified in patients with primary microcephaly and seizures. *J Med Genet,* 42: 725-9, 2005.

SOWELL ER, THOMPSON PM, TESSNER KD, and TOGA AW. Mapping continued brain growth and gray matter density reduction in dorsal frontal cortex: Inverse relationships during postadolescent brain maturation. *J Neurosci,* 21: 8819-29, 2001.

SQUIRE LR, STARK CE, and CLARK RE. The medial temporal lobe. *Annu Rev Neurosci,* 27: 279-306, 2004.

SQUIRE LR, WIXTED JT, and CLARK RE. Recognition memory and the medial temporal lobe: A new perspective. *Nat Rev Neurosci,* 8: 872-83, 2007.

STAHL R, WALCHER T, DE JUAN ROMERO C, PILZ GA, CAPPELLO S, IRMLER M, SANZ-AQUELA JM, BECKERS J, BLUM R, BORRELL V, and GOTZ M. Trnp1 regulates

expansion and folding of the mammalian cerebral cortex by control of radial glial fate. *Cell,* 153: 535-49, 2013.

STANCIK EK, NAVARRO-QUIROGA I, SELLKE R, and HAYDAR TF. Heterogeneity in ventricular zone neural precursors contributes to neuronal fate diversity in the postnatal neocortex. *J Neurosci,* 30: 7028-36, 2010.

SUN T and HEVNER RF. Growth and folding of the mammalian cerebral cortex: From molecules to malformations. *Nat Rev Neurosci,* 15: 217-32, 2014.

SZABO K, FORSTER A, and GASS A. Conventional and diffusion-weighted mri of the hippocampus. *Front Neurol Neurosci,* 34: 71-84, 2014.

SZABO N, PAP C, KOBOR J, SVEKUS A, TURI S, and SZTRIHA L. Primary microcephaly in hungary: Epidemiology and clinical features. *Acta Paediatr,* 99: 690-3, 2010.

TAN CA, DEL GAUDIO D, DEMPSEY MA, ARNDT K, BOTES S, REEDER A, and DAS S. Analysis of aspm in an ethnically diverse cohort of 400 patient samples: Perspectives of the molecular diagnostic laboratory. *Clin Genet,* 85: 353-8, 2010.

TAVERNA E, GOTZ M, and HUTTNER WB. The cell biology of neurogenesis: Toward an understanding of the development and evolution of the neocortex. *Annu Rev Cell Dev Biol,* 30: 465-502, 2014.

THORNTON GK and WOODS CG. Primary microcephaly: Do all roads lead to rome? *Trends Genet,* 25: 501-10, 2009.

VAN DEN BOSCH J. Microcephaly in the netherlands: A clinical and genetical study. *Ann Hum Genet,* 23: 91-116, 1959.

VERLOES A, DRUNAT S, GRESSENS P, and PASSEMARD S. Primary autosomal recessive microcephalies and seckel syndrome spectrum disorders, 2013.

WECHSLER. Adult intelligence scale-iii. *Psychological Corporation, New York*., 1997.

WECHSLER. Wais-iii—wms-iii

The Psychological Corporation. *Harcourt Brace & Co*., *London*., 1998.

WECHSLER. Wechsler intelligence scale for children-iv. *The Psychological Corporation*. *Toronto, Ontario, Canada*, 2003.

WOODS CG, BOND J, and ENARD W. Autosomal recessive primary microcephaly (mcph): A review of clinical, molecular, and evolutionary findings. *Am J Hum Genet*, 76: 717-28, 2005.

FIGURE LEGENDS

Figure 1

Regional differences in brain volume reduction in patients with *ASPM* mutations

(A-E) Quantification of the overall brain volumes in controls and patients. Volumes are expressed as a percentage of the average of the controls. *ASPM* mutations result in regional differences of brain volume reduction between supra and infratentorial compartments (A), brain stem and cerebellum (B), total grey matter and white matter (C), cerebral cortex, subcortical gray matter and cerebellar cortex (D).

Analyses are two-way ANOVAs followed by Bonferroni post hoc tests (# $p<0.05$; ## $p<0.01$; ###: $p<0.001$). Values are group means ±SEM.

Figure 2

Regional differences in cortical volume reduction in patients with *ASPM* mutations

(A-B) Quantification of the cerebral cortical volume in the different lobes in controls and patients (AB). Volumes are expressed as a percentage of the average of the controls. The volume of the cingulate cortex was more reduced than that of the frontal, parietal and temporal lobes in patients as compared to controls, in the right hemisphere (B).

Analyses are two-way ANOVAs followed by Bonferroni post hoc tests (## $p<0.01$; ###: $p<0.001$). Values are group means ±SEM.

(C) Color-coded representation of the cortical volume in patients with *ASPM* mutations, expressed as a percentage of the average of the controls.

The reduction in volume was not uniform throughout the cerebral cortex. Regions in orange to brown indicate those most reduced in volume, i.e. the occipital and cingulate cortices. In contrast, green and yellow regions are those in which patients showed a relative preservation

of their cortical volume, i.e. the parahippocampal and entorhinal cortices and the pars opercularis.

Figure 3

Hippocampal volume is preserved in patients with *ASPM* mutations

(A-B) Example of a 3D "cutaway" view that includes a coronal section and an axial section of the hippocampus in a control subject (A) and in a patient with *ASPM* mutation (B) (as previously shown in (Cho, Han et al.; Dager, Wang et al., 2007; Hopkins, Abildskov et al., 1997; Szabo, Forster et al.), highlighting the volume of the hippocampus in comparison with the rest of the brain (both images are at the same scale).

(C-F) Quantification of the cortical volume in nine regions of the temporal lobes in controls and patients (C, E: bar graph; D, F: individual data presented in a vertical scatter plot). Volumes are expressed as a percentage of the average of the controls. *ASPM* mutations result in regional differences of cortical volume reduction within temporal lobes with preservation of both hippocampi and parahippocampal cortices as well as of the right entorhinal cortex as compared to the other temporal regions.

Analyses are two-way ANOVAs followed by Bonferroni post hoc tests (###: $p<0.001$). Values are group means ±SEM.

Figure 4

Cortical thickness is maintained or increased in patients with *ASPM* mutations

Color-coded representation of the cortical thickness in patients with *ASPM* mutations, expressed as a percentage of the average of the controls, using the same code as for volumetric data.

Cortical regions depicted in dark blue indicate regions with the thicker cortex in patients with *ASPM* mutations as compared to controls, i.e. regions in the dorsolateral cortex lining the Sylvian fissure and the post central sulcus.

Figure 5

The cortical surface area is the most affected parameter in patients with *ASPM* mutations in all regions except in the hippocampus and surrounding medial temporal cortex

(A-B) Quantification of the surface area of the cerebral cortex in the different lobes in controls and patients (AB). Surface areas are expressed as a percentage of the average of the controls. The surface area of the cingulate cortex was more reduced than that of the frontal, parietal, occipital and temporal lobes in patients as compared to controls, in the right hemisphere (B).

Analyses are two-way ANOVAs followed by Bonferroni post hoc tests (##: $p<0.01$). Values are group means ±SEM.

(C) Color code representation of the cortical surface area in patients, expressed as a percentage of the average of the controls. Regions in dark red or brown indicate those most reduced in surface area, i.e. the caudal and rostral middle frontal and rostral anterior cingulate region regions. In contrast, regions in green or yellow are those in which the cortical surface area was more preserved in patients as compared to controls, i.e. the parahippocampal cortices and the right entorhinal cortex.

Figure 6

White matter volume is reduced in similar proportion as the cortex

(A-B) Quantification of the reduction in the volume of the white matter in the different lobes in controls and patients. Volumes are expressed as a percentage of the average of the controls

(C-D) Quantification of the volume of the white matter in the temporal lobes in controls and patients. *ASPM* mutations result in regional differences of white matter volume reduction within the temporal lobe with preservation of the white matter volume of both parahippocampal regions and of the right entorhinal region as compared to the other temporal regions.

Analyses are two-way ANOVAs followed by Bonferroni post hoc tests (#: $p<0.05$; ##: $p<0.01$). Values are group means ±SEM.

Figure 7

Regional differences in Gyrification Index reduction in patients with *ASPM* mutations

Color code representation of the local Gyrification Index in patients, expressed as a percentage of the average of the controls. Regions in yellow are those in which the GI was the lowest in patients as compared to controls, i.e. both pars opercularis and superior temporal regions.

Figure 8

Mnesic abilities of patients with *ASPM* mutations are preserved despite their intellectual deficiency

Cognitive assessment of patients with *ASPM* mutations using Wechsler scales [WAIS III and MEM III (Patients 1 and 2) or WISC IV and CMS (Patients 3 to 5)]. Normal IQ values [115-85] are indicated in dark grey and borderline IQ values [84-70] in light grey. Patients with *ASPM* mutations exhibited mild-to-moderate intellectual disabilities with better performances on long-term memory tests compared to their mean Full scale IQ.

Analyses are one-way ANOVA followed by Bonferroni post hoc tests (***: $p<0.001$). Values are group means ±SEM.

TABLES

Table 1

Molecular and clinical characteristics of patients with *ASPM* mutations

	Refered as in Passemard *et al* 2009	*ASPM* mutations	OFC at birth	Age at the time of evaluation	OFC at the time of evaluation	Cortical dysgenesis	Education and/or career (age)
Patient 1 *	1-2	c.7782_7783delGA homozygous	29cm (-4SD)	24y	47.2cm (-7.5 SD)	0	Sheltered employment in an office (24y)
Patient 2 #	7-1	c.9319+C9507_delG	31cm (-3SD)	20y	47.5cm (-6SD)	0	Sheltered employment as gardener (20y) Reads and writes
Patient 3 *	1-1	c.7782_7783delGA homozygous	32cm (-2SD)	14y	48cm (-4SD)	0	Apprentice baker (at 17y) Reads and writes
Patient 4 #	7-2	c.9319+C9507_delG	31cm (-3SD)	17y	46cm (-6SD)	Right extensive polymicro gyria	Occupational activity Reads and writes with difficulty
Patient 5	3-1	c.6651_6654delAACA homozygous	31,5cm (-2.5SD)	13y9m	47.5 cm (-4SD)	0	Middle school with special educational facilities (13y9m). Reads and writes
Patient 6	10-1	c.2389C>T+c.6686_6689 delGAAA	28 cm (-5SD)	7y	42.5cm (-6SD)	Focal parietal cortical dysplasia	Special educational setting
Patient 7	2-1	c.77delG+c.6232T>C	32cm (-2SD)	8y	42.5 cm (-6SD)	0	Elementary school with special educational setting

OFC = Ocipitofrontal circumference, SD = standard deviation, y = year, m = months
*, # : siblings

*Highlights

Abnormal spindle-like microcephaly-associated (*ASPM*) mutations strongly disrupt neocortical structure but spare the hippocampus and long-term memory

Sandrine Passemard (1-4), Alain Verloes (1-3), Thierry Billette de Villemeur (1,5-6), Odile Boespflug (1,2,4), Karen Hernandez (3), Marion Laurent (7), Bertrand Isidor (8), Corinne Alberti (2,9), Nathalie Pouvreau (3), Séverine Drunat (1, 3), Bénédicte Gérard (3), Vincent El Ghouzzi (1,2), Jorge Gallego (1,2), Monique Elmaleh-Bergès (1,2,10), Wieland B. Huttner (11), Stephan Eliez (12), Pierre Gressens* (1,2,4,13), Marie Schaer* (12,14).

HIGHLIGHTS

- First study of cortical volume/surface/thickness/gyrification in ASPM microcephaly
- *ASPM* mutations disrupt cortical development in a region-specific fashion
- Neocortical volume and surface are reduced by 50%, but with regional variations
- The hippocampus and surrounding medial temporal structures are spared
- There is a corresponding preservation of long-term memory in ASPM patients

Figure 1

Click here to download high resolution image

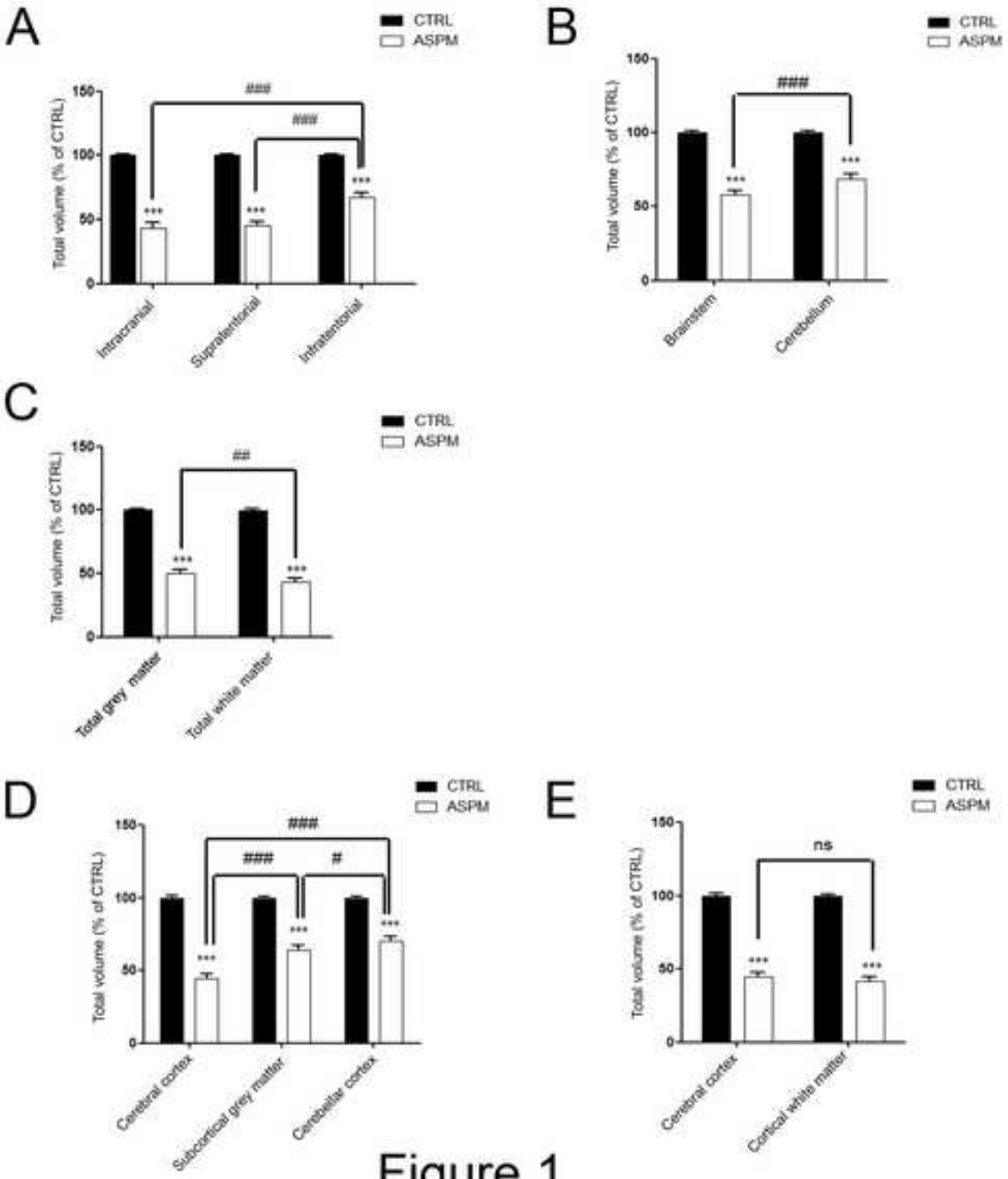

Figure 1

Figure 2
Click here to download high resolution image

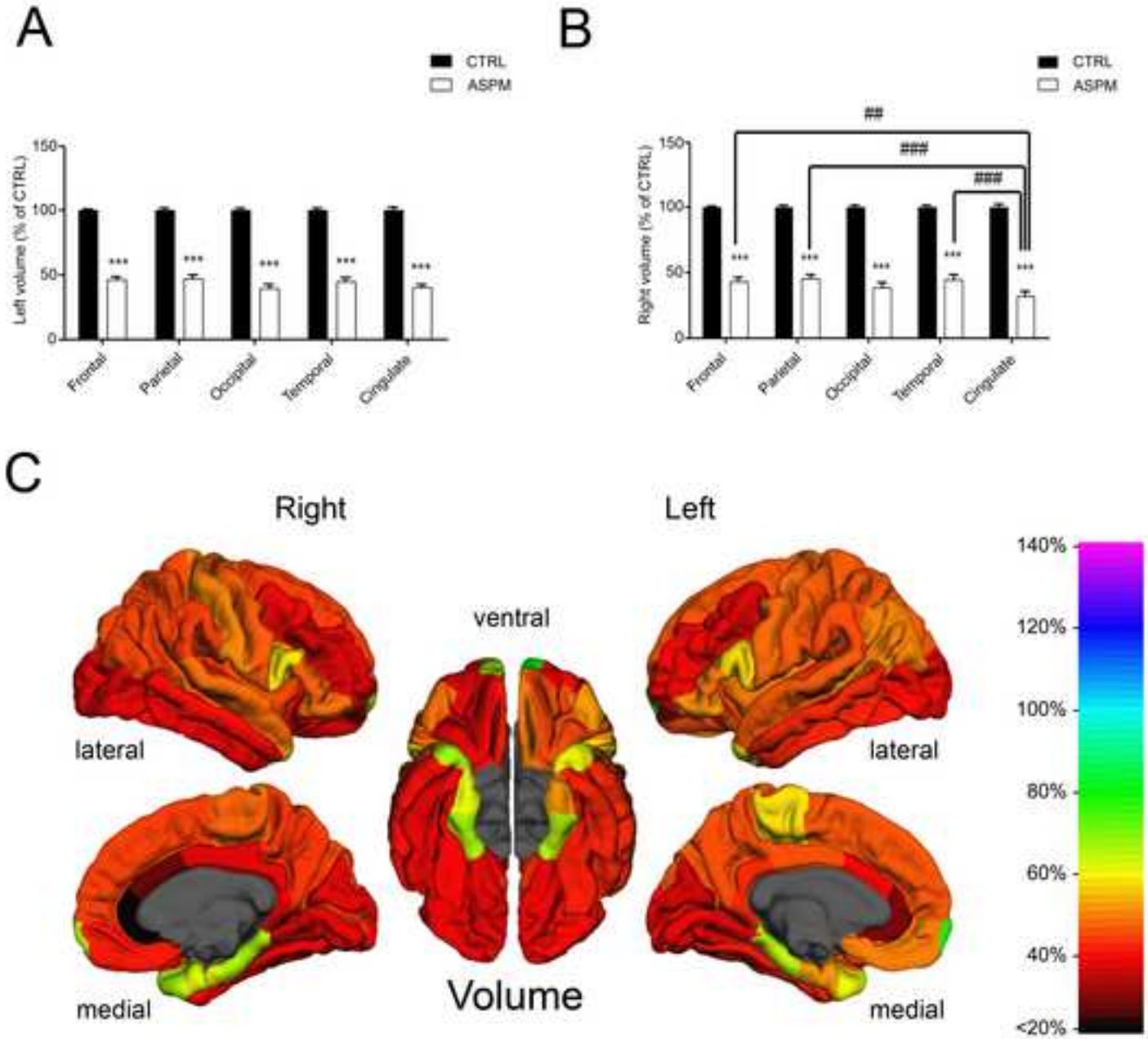

Figure 2

Figure 3
Click here to download high resolution image

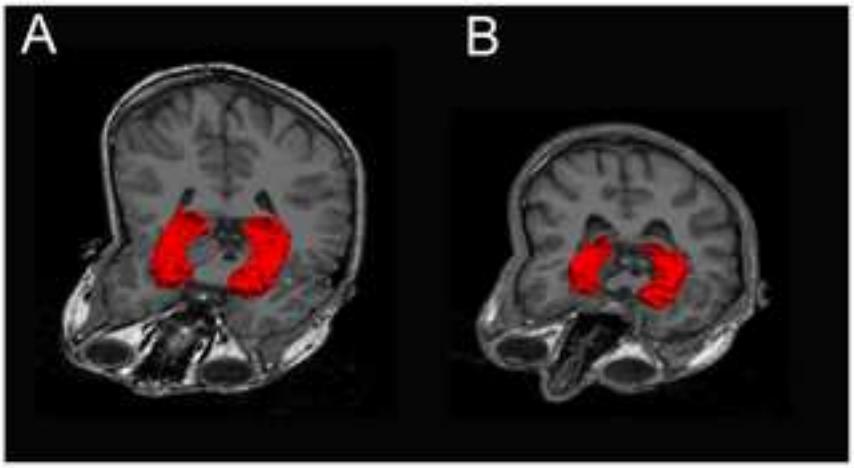

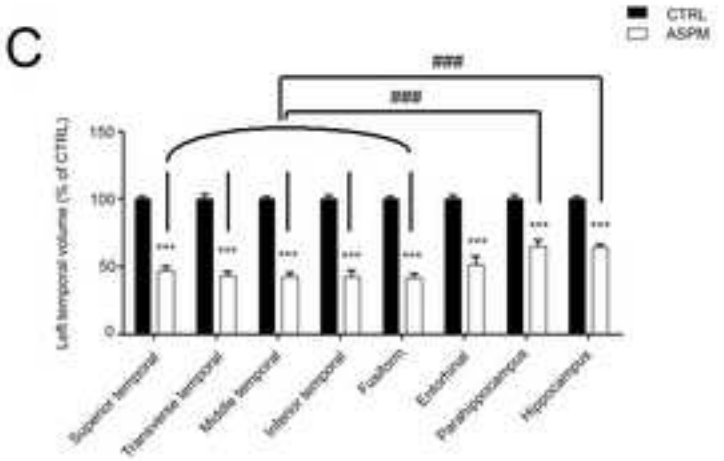

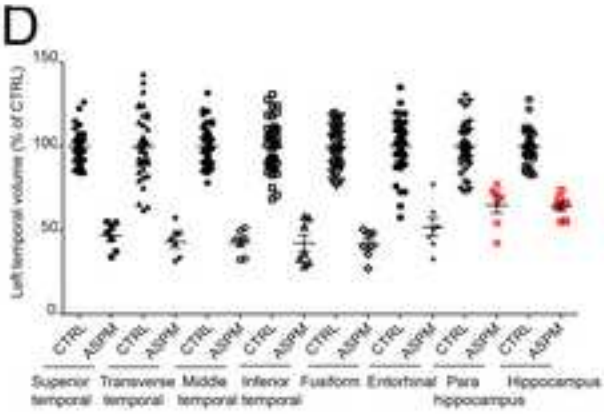

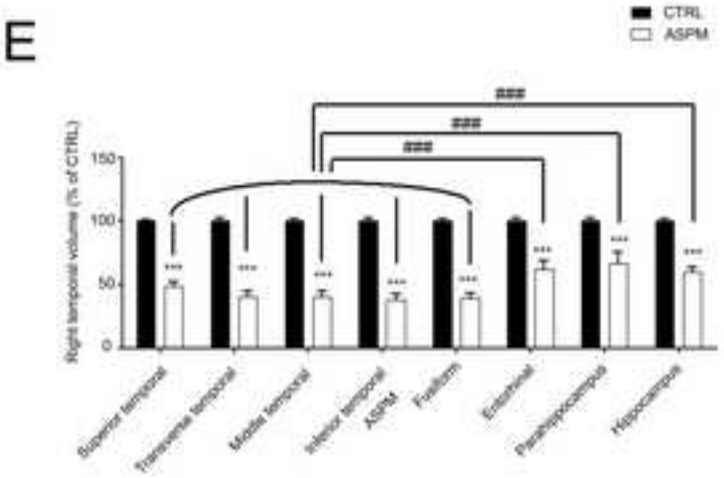

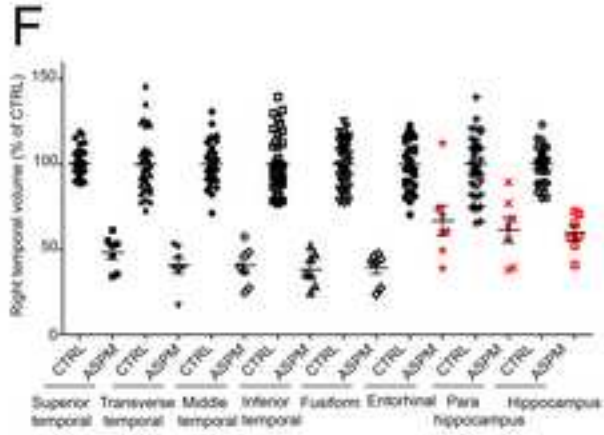

Figure 3

Figure 4
Click here to download high resolution image

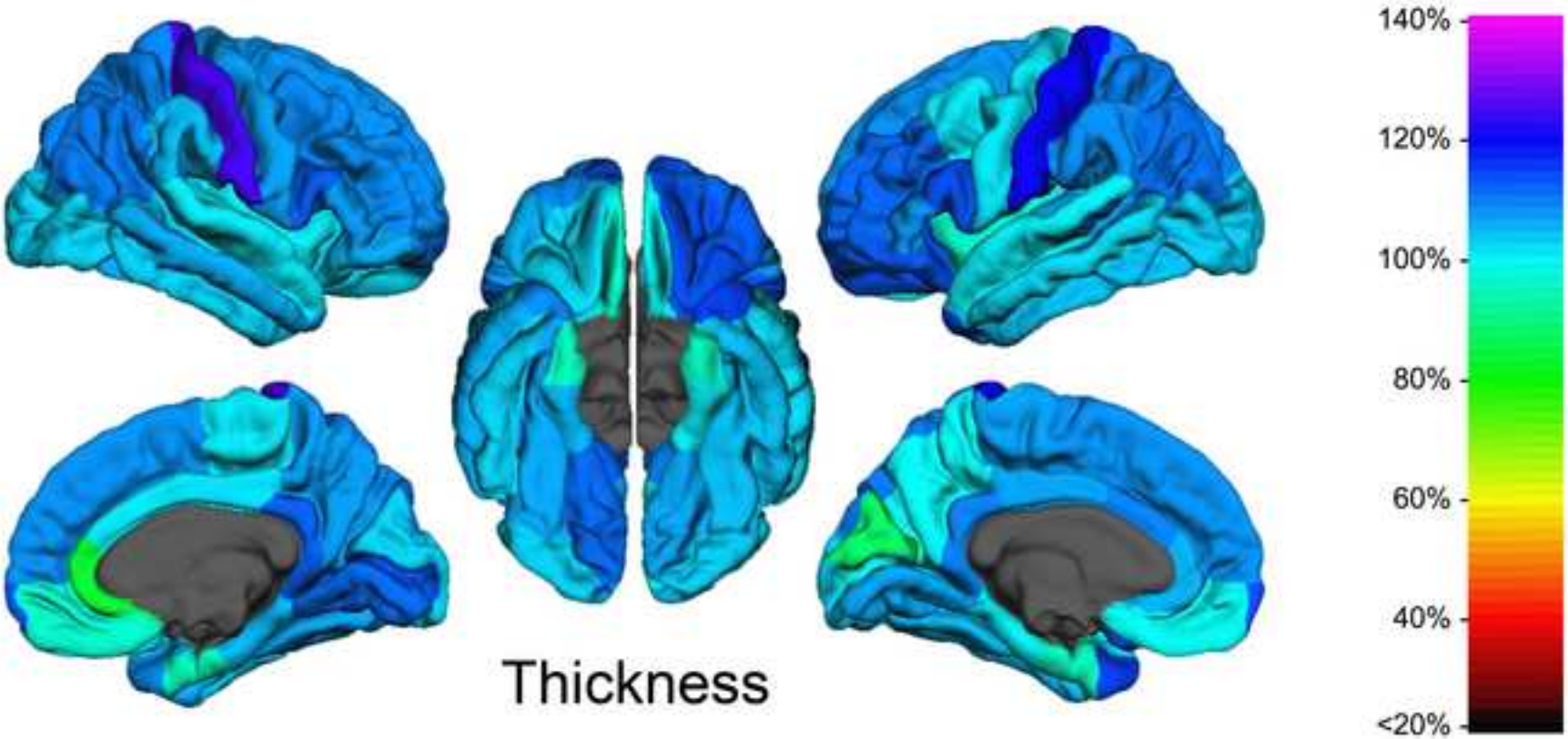

Figure 4

Figure 5
Click here to download high resolution image

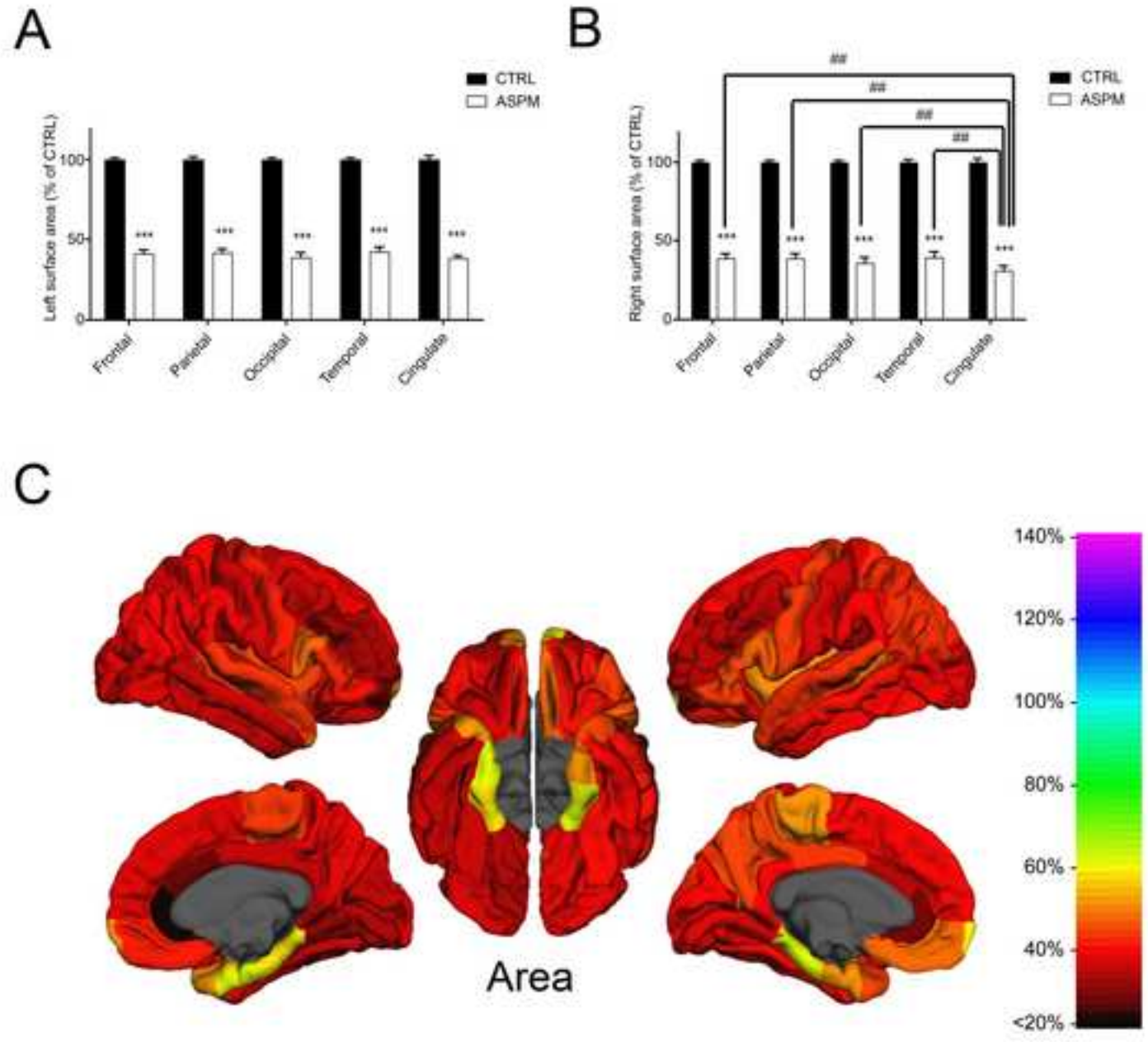

Figure 5

Figure 6
Click here to download high resolution image

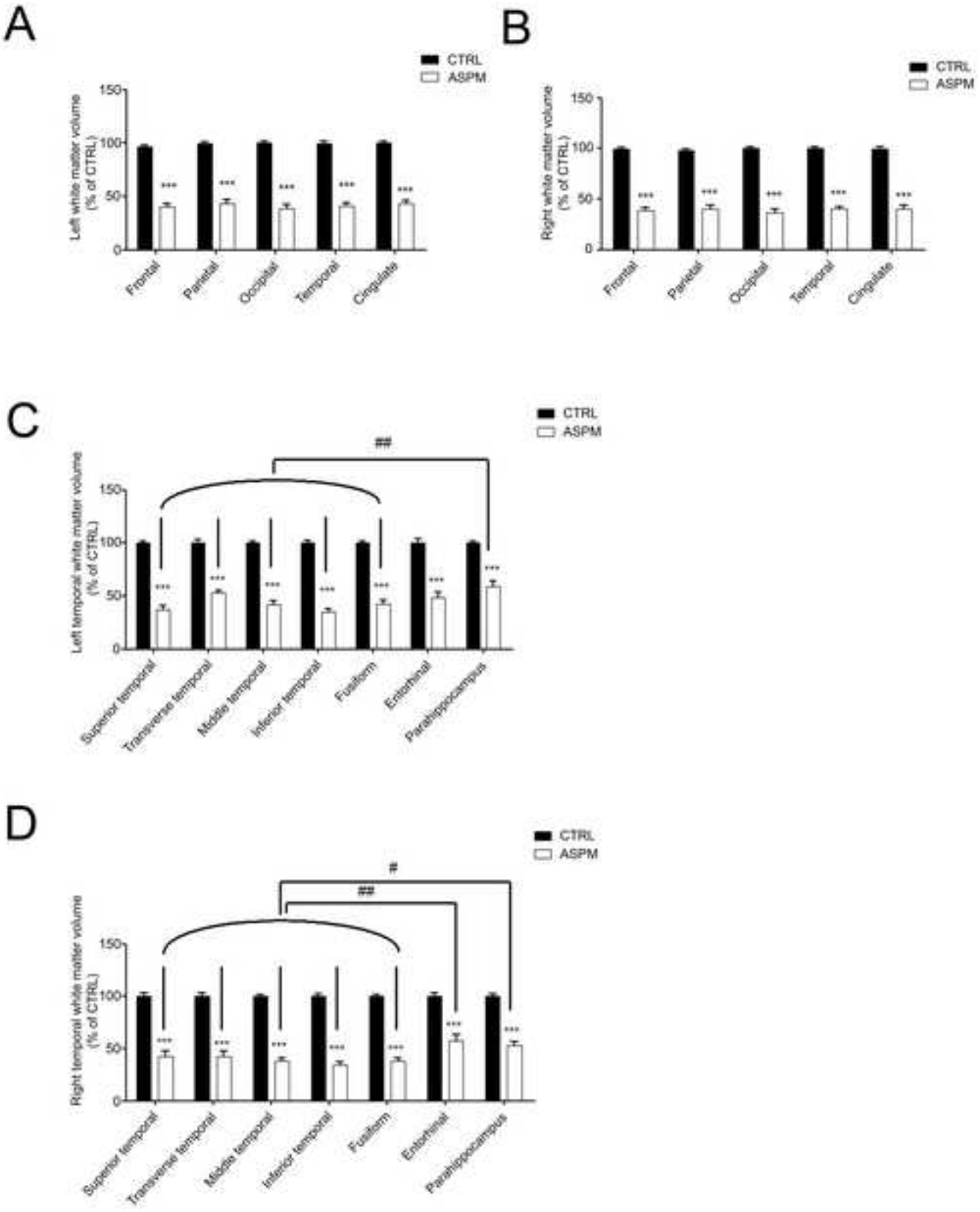

Figure 6

Figure 7
Click here to download high resolution image

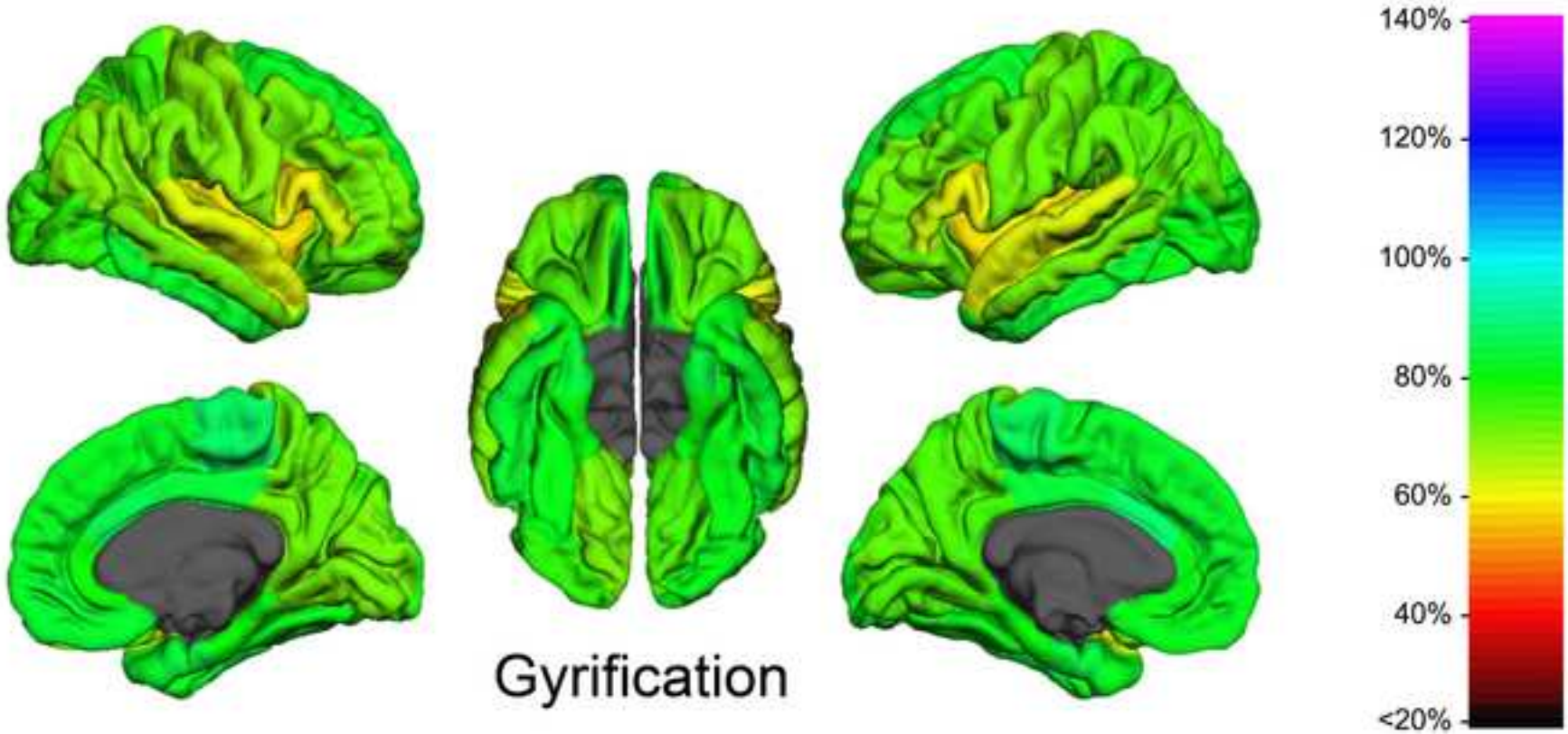

Figure 7

Figure 8
Click here to download high resolution image

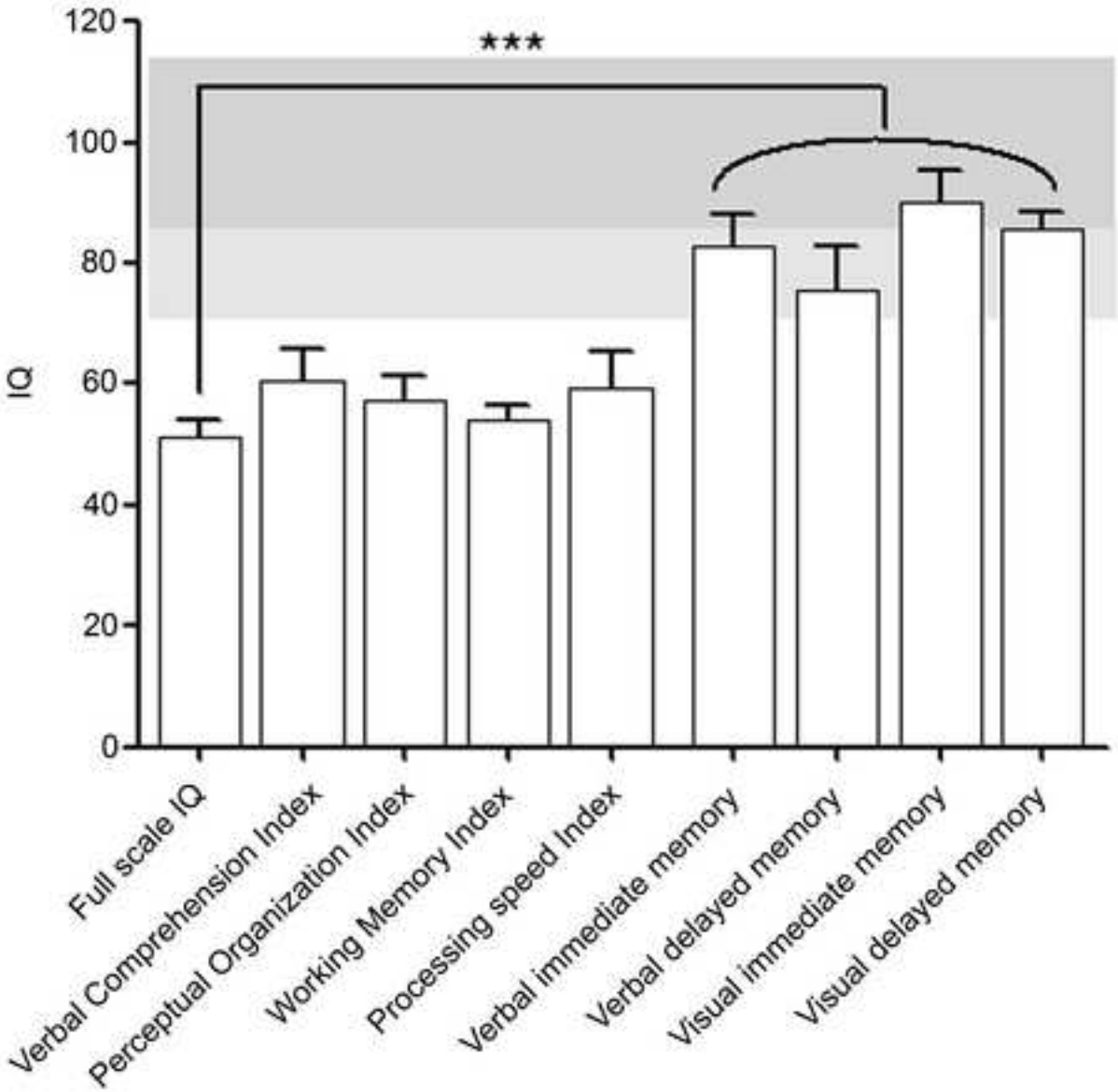

Figure 8